



INTERUNIVERSITY PROGRAMME  
IN  
PHYSICAL LAND RESOURCES

Ghent University  
Vrije Universiteit Brussel  
Belgium



**Potential of soil sensor measurements for soil mapping in Bangladesh**

***Promoter:***

**Prof. dr. ir. Marc Van Meirvenne**

*Master dissertation submitted in partial fulfillment of the requirements for the degree of Master of Science in Physical Land Resources*

***Tutor:***

**M.Sc Mohammad Monirul Islam**

By Md. Noor-E-Alam Siddique

Bangladesh

*Academic Year 2009-2010*



This is an unpublished M.Sc dissertation and is not prepared for further distribution. The author and the promoter give the permission to use this Master dissertation for consultation and to copy parts of it for personal use. Every other use is subject to the copyright laws, more specifically the source must be extensively specified when using results from this Master dissertation.

Gent, August 2010

The Promoter,

The Author,

Prof. dr. ir. Marc Van Meirvenne

Md. Noor-E-Alam Siddique

## **Preface**

The author is grateful to his promoter Prof. dr. ir. Marc Van Meirvenne, Department of Soil Management, Faculty of Bioscience Engineering, for his guidance and support. The lavish cooperation and suggestions from his tutor MSc Mohammad Monirul Islam during the research is highly commendable, spontaneous and appreciable. The author extends his gratitude to the staff members of International Centre for Physical Land Resources, Belgium and Soil Resource Development Institute, Ministry of Agriculture, Bangladesh, for their doctrine and assistance during the study and research period. The financial support of Flemish Inter-University Council (VLIR), Belgian State Secretary of Development Cooperation, is highly acknowledged, without which this academic pursuit would not have been possible.

The author expresses endless gratitude to his parents, wife and only son for their patience sacrifice, support and encouragement during these two years of separation.

Gent, August 2010

Md. Noor-E-Alam Siddique

# Table of Contents

<b>Preface</b>	<b>i</b>
<b>Contents</b>	<b>ii</b>
<b>List of figures</b>	<b>v</b>
<b>List of tables</b>	<b>vii</b>
<b>List of abbreviations</b>	<b>viii</b>
<b>Abstract</b>	<b>ix</b>
<b>1. Introduction</b>	<b>1</b>
1.1 Background	1
1.2 Rationale of the research question	1
<b>2. Review of Literature</b>	<b>5</b>
2.1 Soil spatial variability	5
2.2 Soil sampling: direct method of soil information	6
2.3 Instrumentation for sensed soil information	7
2.3.1 Positioning system	7
2.3.2 Soil sensors	7
2.3.3. Electrical and electromagnetic sensors	8
2.3.4. Eelectromagnetic induction principal and procedure of EM38 sensor	9
2.4. Considerations and limitations for ECa survey	9
2.5 Factors affecting the variability of ECa measurements	10
2.5.1 Texture and other physical properties	11
2.5.2 Soil moisture content	11
2.5.3 Temperature	11
2.7 Geostatistical analysis of spatial data	12
2.8 Soil resource characterization status in Bangladesh	12
2.9 Landuse of Bangladesh	13
<b>3. Materials and Methods</b>	<b>15</b>
3.1 Location	15
<b>3.2 Terrace site</b>	<b>16</b>
3.2.1 Geology of the terrace soils of Bangladesh	16
3.2.2 Hydrology of BT	16

3.2.3 Soil of BT	16
3.2.4 Climate of BT	17
3.2.5 Electromagnetic induction (EMI) survey	17
3.2.6 Soil sampling design	17
3.2.7 Soil physical and chemical analysis	18
3.2.8 Statistical and Geostatistical analysis	19
3.2.8.1 Spatial variation through variography	19
3.2.8.2 Spatial prediction through Kriging	20
3.2.8.3 Ordinary Kriging	21
<b>3.3 Floodplain site</b>	<b>22</b>
3.3.1 Geology of the floodplain of Bangladesh	22
3.3.2 Soil of BF	22
3.3.3 Hydrology of BF	22
3.3.4 Climate of BF	23
3.3.5 Electromagnetic induction (EMI) survey	23
3.3.6 Soil sampling design	24
3.3.7 Soil physical and chemical analysis	24
3.3.8 Statistical and Geostatistical analysis	25
<b>4. Results and discussion</b>	<b>26</b>
<b>4.1 Terrace site</b>	<b>26</b>
<b>4.1.1 Descriptive statistics</b>	<b>26</b>
4.1.1.1 Soil properties	26
4.1.1.2 Apparent electrical conductivity (ECa)	29
<b>4.1.2 Correlation coefficients of ECa with textural and chemical soil properties</b>	<b>30</b>
4.1.2.1 ECa and Texture	30
4.1.2.2 ECa and chemical properties	32
<b>4.1.3 Spatial variability of soil properties</b>	<b>33</b>
4.1.3.1 Mapping of ECa measurements	33
4.1.3.2 Mapping of clay and sand content	35
4.1.3.3 Mapping of chemical properties	38
<b>4.2 Floodplain site</b>	<b>41</b>
<b>4.2.1 Descriptive statistics</b>	<b>41</b>
4.2.1.1 Soil properties	41

<b>4.2.2 Apparent electrical conductivity (ECa)</b>	<b>44</b>
<b>4.2.3 Correlation coefficients of ECa with textural and chemical soil properties</b>	<b>44</b>
<b>4.2.4 Mapping of ECa measurements</b>	<b>46</b>
<b>5. Comparison of EM38 conductivity response with soil properties in the terrace and floodplain site</b>	<b>49</b>
<b>6. Conclusion</b>	<b>50</b>
<b>7. Recommendations</b>	<b>51</b>
<b>8. Reference</b>	<b>52</b>
<b>9. Appendices</b>	<b>58</b>

## List of Figures

Figure 1. General soil types of Bangladesh	3
Figure 2. Soil Physiography map of Bangladesh	4
Figure 3. Picture of EM38 sensor, a) ECa-H orientation and b) ECa-V orientation	8
Figure 4. Diagram showing operation of electromagnetic induction based EM38 sensor	9
Figure 5. Electrical conductivity pathways: 1. Solid-liquid, 2. Liquid and 3. Solid	10
Figure 6. Location of the terrace (Barind Tract) and floodplain sites in the map of Bangladesh	15
Figure 7. The location of (a) terrace study area (2.02 ha), (b) floodplain study area (0.8 ha), google earth image, dated: 31 January 2010	15
Figure 8. Floating Mobile Soil Sensing System during field measurement of ECa; close up views show individually labeled components of the system	23
Figure 9. Histograms of a) ECa-V ( $\text{mS m}^{-1}$ ), b) topsoil clay, c) subsoil clay, d) deepsoil clay e) pH, and f) CEC ( $\text{cmol}^+ \text{kg}^{-1}$ ) in the terrace site	28
Figure 10. Histograms of a) $\text{Ca}^{2+}$ ( $\text{cmol}^+ \text{kg}^{-1}$ ), b) $\text{Mg}^{2+}$ ( $\text{cmol}^+ \text{kg}^{-1}$ ), c) Organic C ( $\text{g kg}^{-1}$ ) d) Base saturation (%) in the terrace site	29
Figure 11. The distribution of a) topsoil, b) subsoil and c) despoil textural class in the USDA texture triangle in the terrace site	30
Figure 12. Scatter plots between ECa-V and a) topsoil, b) subsoil, c) deepsoil clay and d) CEC in the terrace site	33
Figure 13. Variograms of a) ECa-H and b) ECa-V of terrace site	34
Figure 14. Interpolated values in $\text{mS m}^{-1}$ for ECa-H in the terrace site	34
Figure 15. Interpolated values in $\text{mS m}^{-1}$ for ECa-V with sampling locations (shown as dots) in the terrace site	34
Figure 16. Variograms of clay (a, b and c) and sand fractions (d, e and f) in the terrace site	36
Figure 17. Kriged estimates of clay (a, b, c) and sand (d, e, f) content (%) in the terrace site	37
Figure 18. Variograms of a) pH, b) CEC, c) $\text{Ca}^{2+}$ and d) $\text{Mg}^{2+}$ in the terrace site	39

Figure 19. Kriged estimates of chemical properties, i.e., a) pH, b) CEC, c) $\text{Ca}^{2+}$ and d) $\text{Mg}^{2+}$ of topsoil in the terrace site	40
Figure 20. Histograms of a) ECa-H ( $\text{mS m}^{-1}$ ) and b) topsoil clay in the floodplain site	42
Figure 21. The distribution of textural class a) topsoil, b) subsoil and c) despoil in the USDA texture triangle in the floodplain site, n = 20	43
Figure 22. Scatter plots, a) of ECa-H and topsoil clay and b) ECa-V and topsoil clay in the floodplain site	46
Figure 23. Variograms of ECa-H and ECa-V of floodplain site	47
Figure 24. Interpolated values in $\text{mS m}^{-1}$ for ECa-H with a) topsoil clay and c) sand, and ECa-V with b) deepsoil clay contents superimposed on the maps in the floodplain site	48
Figure 25. Relative response of EM38 with depth, in two orientations	58
Figure 26. Schematic showing of the operation of EM38 soil conductivity sensor in vertical dipole mode over deep and shallow topsoil	59

## List of Tables

Table 1. Descriptive statistics of textural fractions in the terrace site, n = 104	27
Table 2. Descriptive statistics of topsoil chemical properties in the terrace site, n = 104	27
Table 3. Descriptive statistics of ECa (mS m <sup>-1</sup> ) measurements in the terrace site	30
Table 4. Pearson correlations (r) of ECa and textural fractions in the terrace site, n = 104	31
Table 5. Pearson correlations of ECa and topsoil chemical properties in the terrace site, n=104	32
Table 6. Model parameters of the fitted omni-directional spherical variograms	34
Table 7. Model parameters of omni-directional spherical variograms for the textural fractions	35
Table 8. Model parameters of omni-directional spherical variograms for chemical properties	38
Table 9. Descriptive statistics of textural fractions in floodplain site, n = 20	41
Table 10. Descriptive statistics of topsoil chemical properties in the floodplain site, n = 20	42
Table 11. Descriptive statistics of ECa (mS m <sup>-1</sup> ) measurements in floodplain site	44
Table 12. Pearson Correlations (r) of ECa and textural fractions in floodplain site, n =20	45
Table 13. Pearson correlations (r) of ECa and topsoil chemical properties, n = 20	45
Table 14. Model parameters of the omni-directional double spherical variograms for ECa	46
Table 15. Loamy to clayey soils of wetland rice crops	62
Table 16. Classes of organic matter (OM) content and cation exchange capacity (CEC)	62
Table 17. Classes of soil reaction	62

## List of Abbreviations

BT	Barind Tract
BM	Brahmaputra Floodplain
ECa	Apparent Electrical Conductivity
ECa-H	Apparent electrical conductivity measured in the horizontal dipole orientation
ECa-V	Apparent electrical conductivity measured in the vertical dipole orientation
EMI	Electromagnetic Induction
FloSSy	Floating mobile sensing system
GIS	Geographic Information System
GPS	Global Positioning System
SRDI	Soil Resource Development Institute, Bangladesh
BARC	Bangladesh Agricultural Research Council
USDA	United States Department of Agriculture
USG	Upazila Soil Guide
FEG	Fertilizer Recommendation Guide
Avil.	Available
Min	Minimum
Max	Maximum
BS	Base saturation
CEC	Cation exchange capacity
Std. dev.	Standard deviation
CV	Coefficient of variation
RNE	Relative nugget effect

## Abstract

An assessment of the field-scale variation of apparent electrical conductivity (ECa) survey and the characterization of correlated soil property was investigated for mapping of a terrace and a floodplain soil of Bangladesh. The electromagnetic induction (EMI) technique was applied by a soil sensor, EM38 which provide ancillary ECa data sets accurately. The survey was supported by soil sampling to assure the reliability and to make evident the potential of ECa measurements for soil mapping. The soils of the study sites greatly differed, the terrace site consisted of a shallow depth clay substratum and the floodplain site bears a sandy substratum. The ECa readings in  $\text{mS m}^{-1}$  ranged from 40 to 64 and 32 to 53 in the vertical (ECa-V) and horizontal (ECa-H) orientation of measurement respectively in the terrace site. In the floodplain site, ECa readings in  $\text{mS m}^{-1}$  ranged from 35.1 to 50.8 and 33.8 to 47.4 for the ECa-H and ECa-V respectively. In the terrace site, the ECa readings correlated best with soil property such as top-, sub-, and deepsoil texture (clay and sand), and topsoil chemical property, i. e., pH, CEC,  $\text{Ca}^{2+}$  and  $\text{Mg}^{2+}$ . For the floodplain site, the ECa readings correlated best with top- and deepsoil texture, and topsoil organic C. A modest correlation was found between ECa-V and the subsoil clay ( $r = 0.78$ ), and ECa-V and the subsoil sand ( $r = - 0.84$ ) in the terrace site. In the floodplain site, the correlation between ECa-H and topsoil clay was the highest ( $r = 0.66$ ). The variogram analysis revealed that a large portion of the total variation of soil property (about 70 %) was accounted by the spatially structured component of the variogram. The study findings have brought an expectation that soil mapping through ECa measurement is possible in Bangladesh. For mapping, the ECa-V measurement in the terrace soil is more predictive than ECa-H while the ECa-H measurement in the floodplain soil is more predictive than ECa-V. The maps of ECa can fairly represent the spatial variation of soil properties. Thus provide useful information on soil texture, chemical fertility and organic matter content. The ECa map also provides a means of monitoring the spatial variation of soil properties that potentially influence the crop production. The ECa maps can also guide directed soil sampling with the purpose of updating the existing soil maps of Bangladesh.

# **1. Introduction**

## **1.1 Background**

Bangladesh is a risk-prone agro-based developing country and is overburdened by the ever growing needs of an exploding population. It has favourable climatic and hydro-edaphic conditions which support intensive agriculture in the alluvium soils of the country. The valuable soil resources of the country are either over-exploited or underutilized because of poor resource management. A land scarce country can hardly afford this. Land use is determined mainly by the monsoon climate and the seasonal flooding which affects the greater part of the country. The high rainfall and seasonal flooding makes conditions particularly suitable for paddy cultivation, and hence paddy occupies about 80 % of the cropped area. Over the past few decades, the conventional agriculture and mono-culture of rice has caused the degradation of agricultural land and the environment due to extensive use of chemical fertilizers and pesticides. Now it is imperative to conduct soil characterization at preferred scale for better understanding and sustainable use of soil resources. The country comprises of three major physiographic units, Holocene floodplain (80 %), Tertiary hills (12 %) and Pleistocene terraces (8 %) with a total land area of 147,570 km<sup>2</sup> (BBS, 2008). The soils have been broadly classified into 19 general soil types (Figure 1) based on similar pedogenic formation and later on, further grouped into 25 physiographic units (Figure 2) (SRDI, 2007; Brammer, 2002). The terrace area representing the second largest agriculturally important land type comprises of the Barind Tract (BT), Madhupur Tract and Akhaura Terrace. Within the BT, three major sub-units can be recognized mostly to the north-west of the country: level BT, high BT and north-eastern BT. The soils of the BT classified as deep and shallow grey terrace soil which are poorly drained, and have a silty topsoil with mottled grey subsoil overlying a Tertiary clay substratum. The level BT occupies about 80 % of BT and consists of 60-90 cm local differences in elevation. The floodplain areas are most important type of landscape in the context of agriculture and culture of the country. The alluvium floodplain is formed by deposits and sediments associated with rivers. Among the floodplains, the Brahmaputra floodplain soil is the second most extensive soil in the country which is 13 % of the total floodplain soils. The soil is silty, imperfectly drained and comprises of non-calcareous dark grey soil having a sandy substratum (Bramer, 2002 and 1996; Saheed, 1992).

## **1.2 Rationale of the research question**

The agricultural activities in the level BT mainly depend on seasonal rains. The soil bears poor natural fertility, low water holding capacity, low structural stability of topsoil and low organic matter with deficiency of plant nutrients, and considered as problem soil of Bangladesh (Bramer, 1996 and USG-Birol, 2008). To find out a suitable combination of agronomic practice to overcome the principal constraint of moisture and fertility various research activities and technology transfer (BMDA, 2010; Orr et. al., 2008; Ali, 2007) are usually found in BT region which intend to increase crop production through cropping intensity and diversification. Food

security and sustained production of BT areas require sufficient inputs, proper management practices and preferred characterization of soils. Therefore, the first study site is selected in BT to characterize the soil which will facilitate implementation of management decisions and optimize input requirements. On the other hand, the majority of agricultural activities concentrate in the floodplain soils which are considered as ever fertile but the fertility scenario has already been changed to a great extent by improper soil management. Now a comprehensive soil management strategy is required which will be capable of maintaining the productivity from agriculture and ensure soil care. Hence, another study site is chosen in Brahmaputra floodplain soil of Bangladesh.

Semi-detail soil survey reports including a thematic polygon map (1:50,000) derived from a conventional survey are available for both the area that belongs to the terrace and floodplain study site. The soils are grouped according to soil series having similar texture, drainage, parent material and use potentials (Saheed, 1992). Due to the lack of quantitative observations, the descriptions about soil attributes are inadequate, and boundaries of such map represent abrupt discontinuity whereas soil attributes are heterogeneous and continuous in nature. Furthermore, spatial variability occurs due to numerous soil processes acting simultaneously, and the prevailing uniform management of fields does not take into account the spatial variability, which is not the preferred way of soil management. Hence, a quick and less expensive method of survey capable of generating quantitative data is required to assess soil spatial variability through detailed soil mapping. This could also be useful to develop a new updating strategy for the existing soil inventory. Geospatial methods such as electromagnetic induction based sensing are capable of producing exhaustive and accurate reliable measurements related to soil attributes over large areas in a rapid and cost effective way. Apparent soil electrical conductivity (ECa) survey information has been widely used to measure various soil physico-chemical properties and subsequent soil mapping (Moral et. al., 2010; Corwin and Lesch, 2005) such as moisture content (Billal, 2008; Sheets and Hendrickx, 1995), and texture, organic matter and CEC (Moral et. al., 2010; Kühn et. al., 2009; Triantafilis and Santos, 2009; Triantafilis et. al., 2009; Sudduth et. al., 2005). The ECa survey measurements provide the basis for detailed soil mapping to investigate the spatial heterogeneity of the soil characteristics. Till to date, such efforts have never been implemented in Bangladesh and there remains a potential of quantitative soil mapping using non-invasive electromagnetic induction soil sensor information for the characterization of the terrace and floodplain soils of Bangladesh.

## **Objectives**

- i. To explore the potential of ECa survey in characterizing soil spatial variability and to assess the value of ECa survey to generate detailed soil property maps for two different soils under paddy cultivation.
- ii. To investigate the nature and extent of correlation of ECa with soil physico-chemical properties and to compare the ECa responses between the investigated sites.

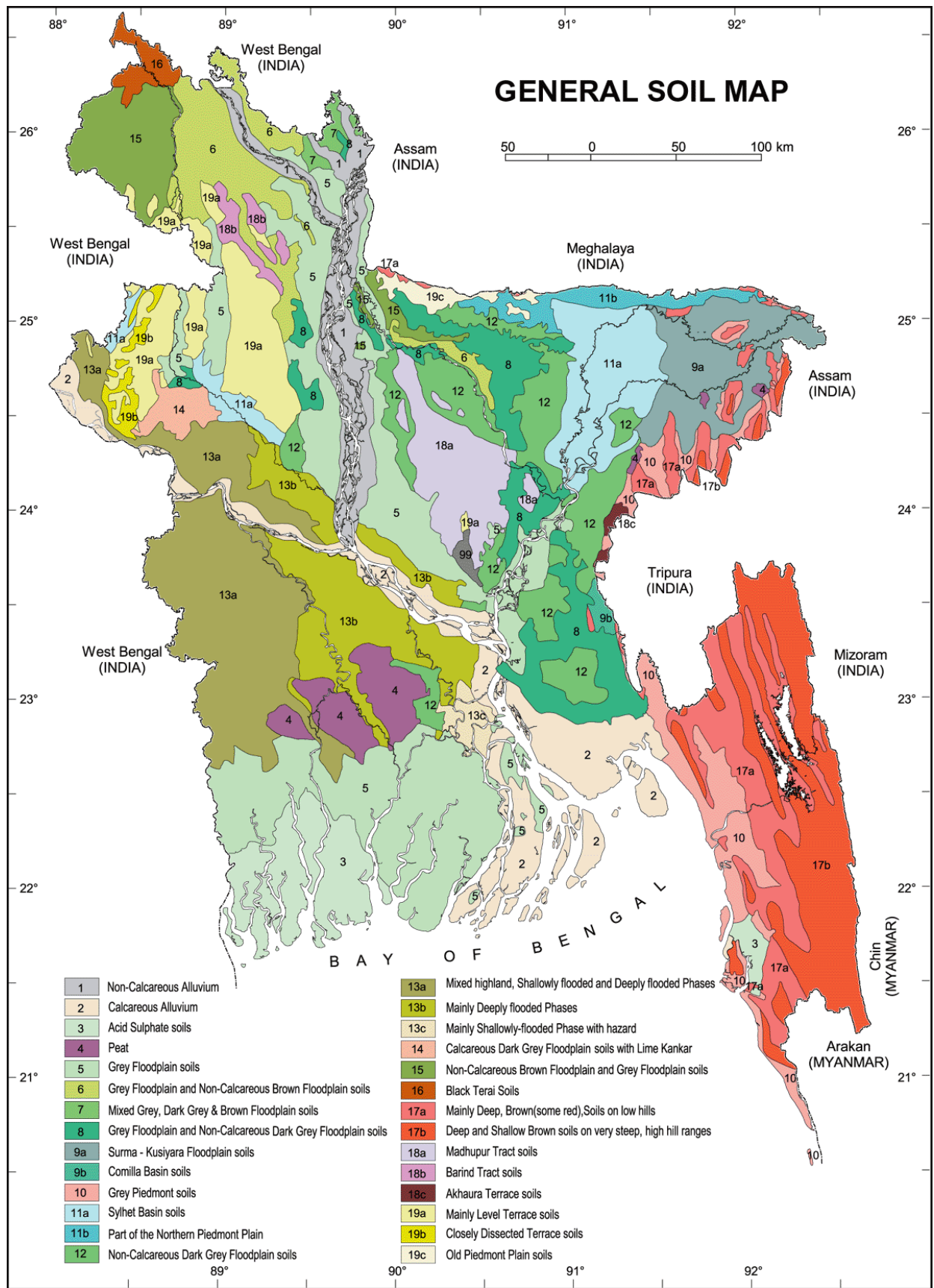


Figure 1. General soil types of Bangladesh (BARC, 2005)

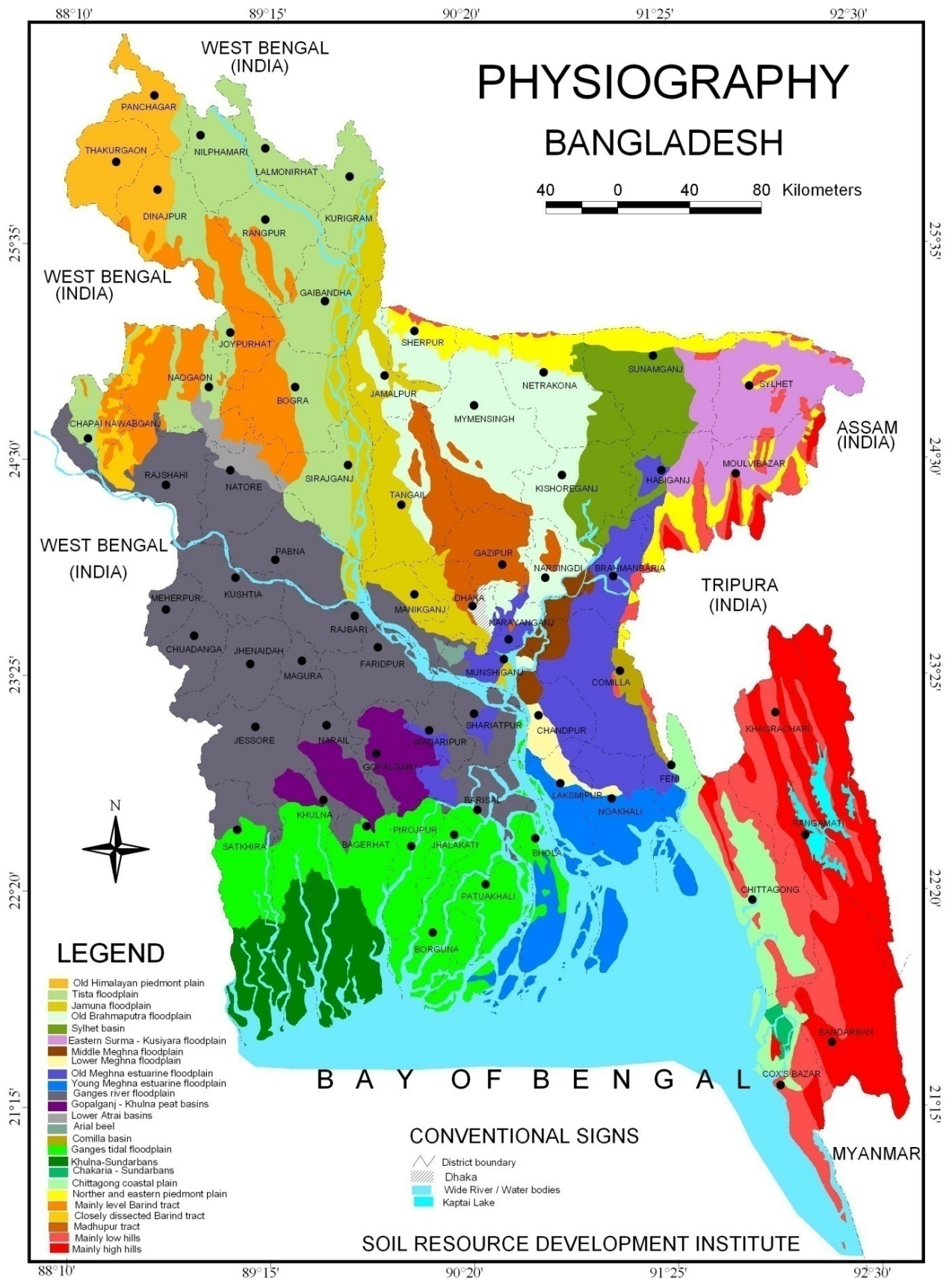


Figure 2. Soil Physiography map of Bangladesh (SRDI, 2007)

## **2. Review of literature**

Soil scientists are aware that soil properties are not static but vary in time and space. Despite of numerous attempts from different context and scale, the characterization of inherently variable soil resources have always been a challenge since soil science has been set out. Sustainable development has reinforced the process to evolve a more quantitative manner to optimize soil management and impart spatially differentiated treatments. These approaches are impelling the cart of classical survey concept apart. As a consequence, new approaches which have caused the development of more time and cost efficient quantitative methodologies for precise characterization of soil variability accurately from exhaustive data. Recent developments make it possible to acquire high resolution data which enable soil mapping at a finer resolution for detail investigations (Cockx, 2010; Kühn et. al., 2009; Viscara et. al., 2008; Vitharana, 2008). The following review aims to provide a conceptual basis to work with the electromagnetic induction soil sensor, EM38 to yield high resolution soil map according to the research objectives.

### **2.1 Soil spatial variability**

The soil varies more or less continuously and many of its properties change continuously from place to place which makes the soil so fascinating. This spatial variability occurs due to the combined effect of physico-chemical and biological processes which operate with different intensities at various scales in soil mantles (Santra et. al., 2008). More specifically, soil variability is influenced by different combinations of soil-forming factors acting through space and time including the additional effects of soil management practices and cropping systems. Generally the magnitude of soil variability increase as the spatial extent and resolution, or time scale increase and after reaching a maximum it stabilize or decrease as space or time dimension continue to increase. The scale of variability could be within-field soil variability over between fields, and landscape to between regions (Lin et. al., 2005). Soil spatial heterogeneity is one of several factors that cause within-field variation in crop yield. Information about soil variability is important in ecological modelling, environmental prediction, precision agriculture and natural resources management (Lin et. al., 2005). Moreover, the characterization of soil variability mainly aims the efficient utilization of agricultural inputs in a cost effective way with respect to spatial variation of soils ensuring environmentally sound use of resources (Santra et. al., 2008). Furthermore, it also provides better understanding of complex relations between soil properties and environmental factors which will enhance the use of soil information in diverse applications. There have always been continuous efforts by the scientist to identify the soil variability at various scales. Earlier, soil surveyors tried to map the soil with a conceptual model of soil variation depending on landform, geology, vegetation and land use. This approach escaped the spatial variability within map units for a variety of reasons including scale limitations and inadequate quantitative data (Soil Survey Division Staff, 1993). The inability of conventional farming to address within-field variations not only has a detrimental economic impact due to

reduced yield in certain areas of a field but also adversely affects the environment due to over applications of inputs. Later, the need of sustainable management of soil resources appeals for an alternative approach which will substantially increase the productivity and resource efficiency, and desirable in the ecological context. The quantification of soil variability could be achieved through direct information (soil sampling) and or sensed information by soil sensors as EM38 (Cockx, 2010). Featuring soil variability on a field scale through dense apparent electrical conductivity (ECa) measurements are increasingly being used in precision agriculture which requires the delineation of site-specific zones to describe the spatial variation of soil properties (Cockx, 2010; Vitharana, 2008; McBratney et. al. 2005; Corwin and Lesch, 2003).

## **2.2 Soil sampling: a direct method of soil information**

A soil sampling strategy depends on the extent and nature of management objectives. It could be a grid sampling, random sampling or continuous sampling. Grid soil sampling is a procedure used to obtain an unbiased assessment of the variability that exists in a field. It involves laying grids which may be specific or range of sizes over the fields, and sampling from each grid cells. With this type of sampling higher sampling density could be attempted for finding intensive variability of soil attributes in some part of a management area. The sampling point could be of the centre of the grid, random within each grid cell or targeted sampling based on non uniform field characteristics (Wollenhaupt et. al., 1997). While random sampling can be divided into simple and stratified random sampling. Simple random sampling is appropriate when the entire population from which the sample is taken is homogenous and for stratified random sampling the population is divide into a number of parts or ‘strata’ according to some characteristics. Stratified sampling techniques are generally used when the population is heterogeneous, where certain homogeneous, or similar, sub-population can be isolated as strata. An alternative sampling scheme that aims to reduce the number of sampling sites and hence labour and costs is termed ‘zone or direct sampling’. It is based on dividing fields into smaller units (or strata) based on fine scale data such as yield, proximal soil sensors, remote sensing or digital elevation models. Sampling is then performed within each zone depending on the variability present. However, several old and new soil sampling techniques allow for measuring soil properties at a range of accuracies and spatial scale. Soil coring is the most direct and accurate method to obtain information about soil texture and horizon but it is the most expensive method for sampling over a large area requiring large number of samples (Zhu et. al., 2004). Researchers have been looking for non-destructive or indirect alternatives to soil coring and have developed several new techniques such as on-the-go soil sensing systems for continuous sampling which refers to the practice of collecting samples directly measuring the variables from the fields.

## **2.3 Instrumentation for sensed soil information**

### **2.3.1 Positioning system**

A fundamental element for locating soil information is the need to accurately determine positions on the ground which is achieved with a global positioning system (GPS). The GPS is used to provide such information which is vital in predictive or detailed soil mapping. This georeferencing allow to analyze relationships among data based on their geographic locations and this spatial technique implies a new way of looking at agricultural information and site variability (Stafford, 2000).

### **2.3.2 Soil sensors**

Soil information obtained using invasive and non-invasive sensors have proven to be useful for monitoring spatial and temporal variability of soil. Invasive methods require a direct contact with the soil to obtain measurements where non-invasive methods provide estimates of soil properties at various depths without direct contact. Viscarra Rossel and McBratney (1998) first suggested the term ‘proximal sensing’ to describe devices that are able to collect data from a distance that is in close proximity to the object of interest. Proximal sensors are capable of gathering data intensively so that properties may be determined continually and almost continuously. Non-invasive proximal soil sensors provide estimates of soil condition at various depths from above ground observations while invasive sensors disrupt the soil surface and penetrate the soil to either sense directly or collect soil for external detection. Both type of sensors can be inter-phased with a GPS receiver and attached to a vehicle to obtain geo-referenced measurements on-the-go. These sensors provide exhaustive soil information which serve as a proper start for an accurate characterization of soil spatial variation. Some of these sensors are capable of directly measuring the soil properties and others provide ancillary or secondary information to estimate soil properties (Vitharana, 2008). However, Erickson (2004) noted several types of soil sensor according to their following applications:

- i. Electrical and Electromagnetic: soil texture, soil moisture, soil depth variability (depth of topsoil, depth to hardpan), and cation exchange capacity (CEC)
- ii. Optical and Radiometric: organic matter, soil moisture, mineral Nitrogen and Phosphorus
- iii. Acoustic and Pneumatic: soil texture, soil bulk density (compaction) and depth variability
- iv. Mechanical: soil compaction, depth of hardpan, mechanical resistance and metal-friction
- v. Electrochemical: soil pH, residual Nitrogen, Sodium and Potassium content

Proximal soil sensing techniques must be developed strategically to meet the demand for high-resolution soil data. Recently a number of field-deployed proximal sensing systems for on-the-go measurements have been developed and are commercially available (Triantafilis and McBratney, 1998). The apparent electrical conductivity ( $EC_a$ ) measurement is particularly well suited for

establishing within field spatial variability of soil properties because of its quick, easy and reliable measurement. The development of mobile  $EC_a$  measurements has made it possible to produce an  $EC_a$  map with measurements taken every few meters. Furthermore, soil sensing systems include several advantages such as elimination of costly and tedious sampling and analysis, efficient acquisition of fine spatial resolution, real-time availability of results, minimal sample handling and elimination of laboratory induced variability (Raphael, 2002).

### 2.3.3. Electrical and electromagnetic sensor

Electrical and electromagnetic sensors use electric circuits to measure the capability of soil particles to conduct or accumulate electrical charge. The soil becomes part of an electromagnetic circuit and the changing local conditions immediately affect the signal recorded by a data logger. The ability of the soil to conduct electricity is usually quantified by electrical conductivity or electrical resistivity. Non-contact  $EC_a$  measurement can be accomplished using a pair of inductors. When a transmitting coil with alternating current is placed in proximity to the soil, the magnetic field induces a flow of electrical charge in the soil. This current is sensed using a receiving coil also placed in proximity to the soil. The distance between two coils and their orientation defines the effective measurement depth. Several commercial implements have been developed and marketed that utilize this method for on-the-go measurement. For example, one way to estimate soil electrical conductivity is by electromagnetic induction using Geonics Limited EM38 sensor (Figure 3).



Figure 3: Pictures of EM38 sensor, a)  $EC_a$ -H orientation and b)  $EC_a$ -V orientation

The EM38 has a transmitting coil which induces a magnetic field that varies in strength with soil depth. A receiving coil measures the primary and secondary induced currents in the soil and relates the two to the soil electrical conductivity (Figure 4). Rapid response, low cost and high durability have made electrical and electromagnetic sensors the most attainable techniques for on-the-go soil mapping. Obtained maps have been correlated to soil texture, salinity, organic matter, CEC, moisture content and other soil attributes (Adamchuk et. al., 2004). Operation

speed and height, soil moisture and temperature, topsoil depth and simply instrumentation drift with time may cause significant effects on EC<sub>a</sub> measurements while using an electromagnetic soil sensor (Sudduth et. al., 2001).

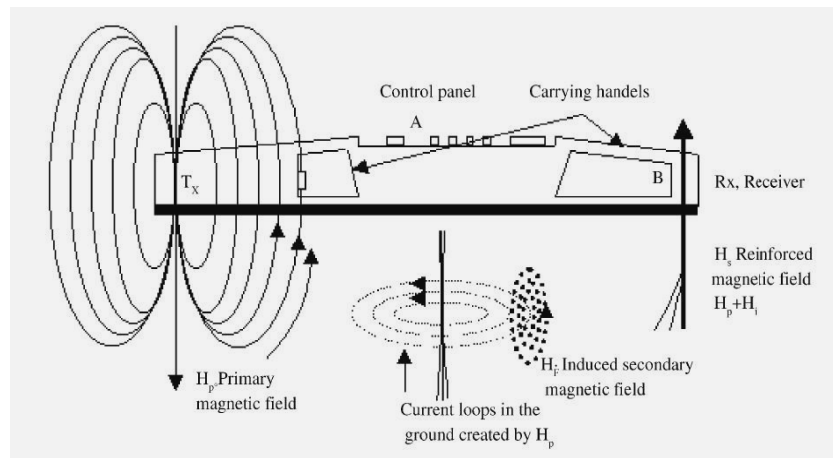


Figure 4. Diagram showing operation of electromagnetic induction based EM38 sensor (Robinson et. al., 2004).

### 2.3.4 Electromagnetic induction (EMI) principal and procedure of EM38 sensor

The EMI principal and procedure has been described in Appendix I.

### 2.4 Considerations and limitations for EC<sub>a</sub> survey

The basic elements of a field-scale EC<sub>a</sub> survey for application include: (i) EC<sub>a</sub> survey design, (ii) geo-referenced EC<sub>a</sub> data collection, (iii) soil sample design based on geo-referenced EC<sub>a</sub> data, (iv) soil sample collection, (v) physico-chemical analysis of pertinent soil properties, (vi) if soil salinity is a primary concern of a stochastic or deterministic calibration of EC<sub>a</sub> to soil sample-determined salinity by the electrical conductivity of the saturation extract, (vii) spatial statistical analysis, (viii) determination of the dominant soil properties influencing the EC<sub>a</sub> measurement at the site of interest and (ix) GIS development (Corwin and Lesch, 2005).

Even though surveys of EC<sub>a</sub> are a quick, reliable and cost-effective means of characterizing spatial variability of a variety of physico-chemical properties, there are limitations too. Measurements of EC<sub>a</sub> by themselves do not directly characterize soil spatial variability. EC<sub>a</sub> measurements provide limited direct information about the physico-chemical properties that influence yield or determine soil quality. Rather, EC<sub>a</sub> survey measurements provide the spatial information necessary to direct soil sampling. It is as a cost-effective tool for directing soil sampling that EC<sub>a</sub> survey measurements are invaluable for characterizing spatial variability. Furthermore, EC<sub>a</sub> directed soil sampling can only spatially characterize soil properties that correlate with and are measured by EC<sub>a</sub>. Apparent soil electrical conductivity is a complex

measurement that requires knowledge and experience to interpret. Soil samples are obligatory to be able to understand and interpret spatial measurements of EC<sub>a</sub>. Without ground-truth soil samples an EC<sub>a</sub> survey will be of minimal value. Spatial measurements of EC<sub>a</sub> do not supplement the need for soil sampling but they do minimize the number necessary to characterize spatial variability. Users of EC<sub>a</sub>-survey data must exercise caution and be aware of what EC<sub>a</sub> is actually measuring at the site of interest (Corwin and Lesch, 2005). EC<sub>a</sub> is not a tool that can completely replace a trained soil survey specialist rather it has the potential as a soil survey tool in situations where field contain soils with large ranges of EC<sub>a</sub> values. In respect to soil mapping purposes, well trained personnel in both soil survey and the theory behind the use of EC<sub>a</sub> instrumentation is a prerequisite. The dense EC<sub>a</sub> survey information might not work for soil mapping in all situations and the individual interpreting EC<sub>a</sub> results for soil mapping applications needs to have an understanding of the soils being mapped prior to interpreting EC<sub>a</sub> results (Brevik et. al., 2006).

## 2.5 Factors affecting the variability of EC<sub>a</sub> measurements

Variation of EC<sub>a</sub> within a field is due to spatial variation in soil properties influencing EC<sub>a</sub>. It varies due to gradations in salinity, clay content and mineralogy, texture, cation exchange capacity and water content through the soil profile and soil temperature (McNeill, 1980). In addition, for the soils in humid climate which contain negligible amount of salts, there the spatial variation in the EC<sub>a</sub> signal is mainly controlled by clay content and associated mineralogy (Lesch et. al., 2005; Auerswald et. al., 2001). Apparent soil electrical conduction in sufficiently moist soils is primarily via salts contained in soil water occupying the larger pores; consequently, measurement of EC<sub>a</sub> of bulk soil is closely related to soil salinity. However, there is also a contribution by the solid phase to EC<sub>a</sub> in moist soil primarily via the exchangeable cations associated with clay minerals. Another pathway exists through soil particles in direct and continuous contact with one another (Rhoades et. al., 1999). These three pathways of current flow contribute to the EC<sub>a</sub> readings (Figure 5).

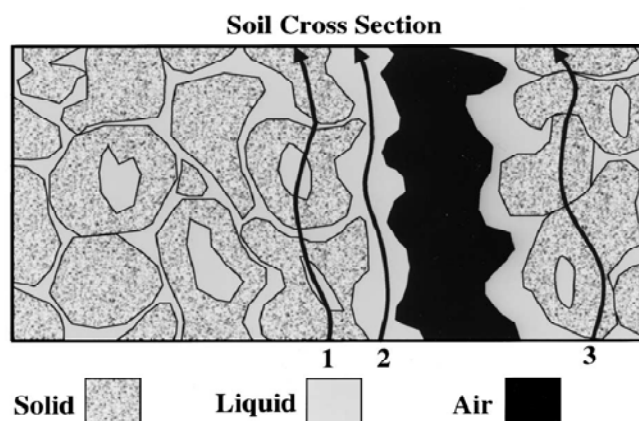


Figure 5. Electrical conductivity pathways 1. Solid-liquid, 2. Liquid and 3. Solid (modified from Rhoades et. al., 1989)

### **2.5.1 Texture and other physical properties**

Soil texture can cause extremely complex spatial patterns of ECa. Under a uniform irrigation distribution, water content will generally coincide with texture. Minimal complexities in spatial patterns of ECa occur when there is minimal soil texture variability. This also happens when the texture changes are smooth and gradual across the field or when the texture, water content and salinity variations are strongly correlated. Non-spherical particle shapes and broad particle-size distributions tend to decrease ECa. Other physical properties also affect the ECa survey readings to various degrees including magnetic susceptibility especially when soils high in free iron oxides, ionic composition of soil solutes, topsoil structure and bulk density (Waller et. al., 2007; Corwin and Lesch, 2005; Schumann and Zaman, 2003).

### **2.5.2 Soil moisture content**

Soil water content is another dynamic soil property that varies with depth and across the landscape, generally with moderate to high local-scale variability which affects ECa measurements. Brevik (2006) reported that for over 50 % of the variability in soil ECa reading caused by moisture and help to anticipate the magnitude and range of ECa readings expected from a given soil. It is important to remember that if the water content of the soil drops too low, the EM readings can become seriously dampened. Reliable EM signal data will be obtained when the soil is moist, or near or at field capacity. Agronomic practices like irrigation management has a pronounced effect on ECa distributions within a field as the leaching fraction and irrigation water quality are affecting the soil water content (Benson et al., 1997; Corwin et. al., 2006). Furthermore, Surface topography plays a significant role in influencing spatial ECa variation. Slope and aspect will determine the level and location of runoff and infiltration, which will influence the variation in water content and salinity at local scales and larger. In addition, another source of potential ECa variation arises from soil compaction caused by repetitive traffic patterns of heavy agricultural equipment (Corwin and Lesch, 2005).

### **2.5.3 Temperature**

With respect to temperature, a 1 °C change in temperature throughout the entire soil profile typically causes no more than a 2% change in the EM-38 signal readings. Since soil temperature fluctuations below 0.3 m in the soil profile occur rather slowly, the entire survey process can usually be completed before a significant change in the bulk average soil profile temperature occurs. In addition, care should be taken when transforming the field-measured ECa values to the ECa at a reference temperature (25 °C) (Sheets and Hendrix, 1995).

However, there are many factors that affect ECa still Friedman (2005) summarized these into three categories: a) the bulk soil and the respective volumetric fractions occupied by the three phases and possible secondary structural configurations (aggregation): porosity, water content

and structure, b) second category are the important solid particle quantifiers which are relatively time-invariable: particle shape and orientation, particle-size distribution, cation exchange capacity (CEC), wettability and, c) factors related to soil solution attributes which change quickly in response to alterations in management and environmental conditions - the ionic strength, cation composition and temperature. Furthermore, the author discussed the roles of the various geometrical and interfacial attributes of the soil and its solution, in determining the effective electrical conductivity of the soil and noted that the soil salinity and the soil volumetric water content are the main factors affecting the soil ECa, the dependence on water content being stronger always.

## **2.7 Geostatistical analysis of spatial data**

The statistical analysis starts with an exploratory data analysis to verify the correctness of the acquired data and also to get familiar with the different data sets which could be obtained from soil sample or with a soil sensor. The term `Geostatistics` refers to the statistical analysis of phenomena which vary in a spatial continuous way. Geo-referenced observations are almost always correlated to some degree in relationship with the distance between the observations. This corresponds to the intuitive feeling that places close to one another tend to have more similar values than the ones further apart. Geostatistics often consists of variography and kriging. Variography uses semivariograms to characterize and model the spatial variance of the data, whereas kriging uses the modeled variance to estimate values between samples. The scale of spatial variation of variables and spatial prediction through estimating the values of a target variables at unsampled location is determined which is also referred to as spatial interpolation or mapping (Hengl et. al., 2004). Geostatistical analysis methods have been proven to be useful for characterization and mapping spatial variation of soil properties and have been received increasing interest by soil scientists and agricultural engineers in recent years (Webster and Oliver, 2001; Corwin and Lesch, 2005).

## **2.8 Soil resource characterization status in Bangladesh**

Bangladesh is a relatively information rich country regarding land and soil resources. It has reconnaissance (written in English) and semi-detail (1:50,000) conventional soil survey reports and maps (prepared in Bangla) for the whole country. Brammer (2002) mentioned that because of the amount of information collected, the survey was more detailed than the term reconnaissance sometimes indicates, while the semi-detail survey report currently is used for national and local level planning in agriculture and management decisions. The Soil Resource Development Institute (SRDI), the erstwhile Department of Soil Survey, carried out reconnaissance soil surveys yielding a total of 34 volumes. The survey approach was based on intensive aerial photo interpretation, followed by field examination of soils along planned

transverses of the landscapes. The USDA 'Soil Survey Manual' was used for describing the soil and map units. The soils had been tentatively correlated with the USDA *Soil Taxonomy* (Soil survey staff, 1993) and also with the FAO-UESCO soil legend (FAO-UESCO, 1988). However, soil classification was supported by physical and chemical analytical data. Soils were mapped in terms of geographical associations or complexes of soil series and phases. Reports include a somewhat detail account of soils, their relationships with the environment and existing land use and their development potentials and constraints. Maps on soil associations and land capability associations at 1:125,000 scale and land use associations at 1:500,000 scales are provided. Reconnaissance soil surveys identified 483 soil series and 38 miscellaneous land types, occurring in 28 map subunits distributed over the major physiographic units, i. e., Floodplain, Pleistocene terrace and Tertiary hills (SRDI, 1986).

During the period 1984-1992, semi-detailed survey was carried out throughout the country for determination of soil nutrient status by chemical analysis of composite topsoil samples, interpretation, fertilizer recommendation, land use pattern and specify required doses of crop specific fertilizer. This intensive and voluminous work finally yielded 'Land and Soil Resource Utilization Guide' or Upazila Soil Guide (USG) for each districts of the country. The map of the guide was produced at the 1:50,000 but no spatial distribution could be shown in those maps. The adapted legend includes land types, soil series and group, soil color, soil texture, soil consistence, soil reaction, drainage condition, and indication of thermal and agro-ecological zones within an Upazila (lowest administrative tier). The potentialities of this resource have not been exploited thoroughly due to lack of extension activities, planning and retarded updating activities (Saheed, 1992).

## **2.9 Landuse of Bangladesh**

Landuse of the country is determined mainly by the monsoon climate and the seasonal flooding through rain which affects the greater part of the country. These physical determinants are reinforced by high population pressure, and by alterations to the natural environment through flood protection, drainage and irrigation interventions changing the evergreen mantle of Bangladesh. Floodplain settlements typically are concentrated on the higher land which is surrounded by agricultural land extending down to the lower land which is most deeply flooded in the moonsoon season. Thus, the agricultural land around a 'typical village' comprised of a range of soil, and depth of flooding, land types, and so do the farmer's fragmented land holdings throughout the country.

Bangladesh climate makes conditions suitable for growing tropical crops such as rice and jute in the warm rainy season, temperate crops such as wheat, corn and potato including pulses, oilseeds in the cool winter months, and sub-tropical crops such as sugarcane and banana throughout the year. More than 50 different crops are grown in Bangladesh. However, the high rainfall and

seasonal flooding makes conditions particularly suitable for paddy cultivation, and hence rice occupies about 80 % of the cropped area. There are two main cropping seasons (Kharif and Rabi) and three rice-growing seasons (Aus, Transplanted Aman rice and Boro - spring rice). The Kharif season comprised of an early part (pre-monsoon and early moonsoon) when Aus paddy and jute are principal crops, and a later part (second half of the moonsoon season and early post-monsoon) when transplanted Aman paddy is the principal crop, deep water Aman paddy is sown pre-monsoon and harvested post-monsoon. Much land produces two crops a year except some part of the Barind Tract (BT), and some produces three (even four) crops (Brammer, 2002).

### 3. Materials and Methods

#### 3.1 Location

The terrace study site lies between latitude 25° 39' 29" N and longitude 88° 35' 44" E in Dinajpur district and the floodplain site lies between latitude 24° 43' 11.68" N and longitude 90° 25' 35.58" E in Mymensingh district in Bangladesh (Figure 6).

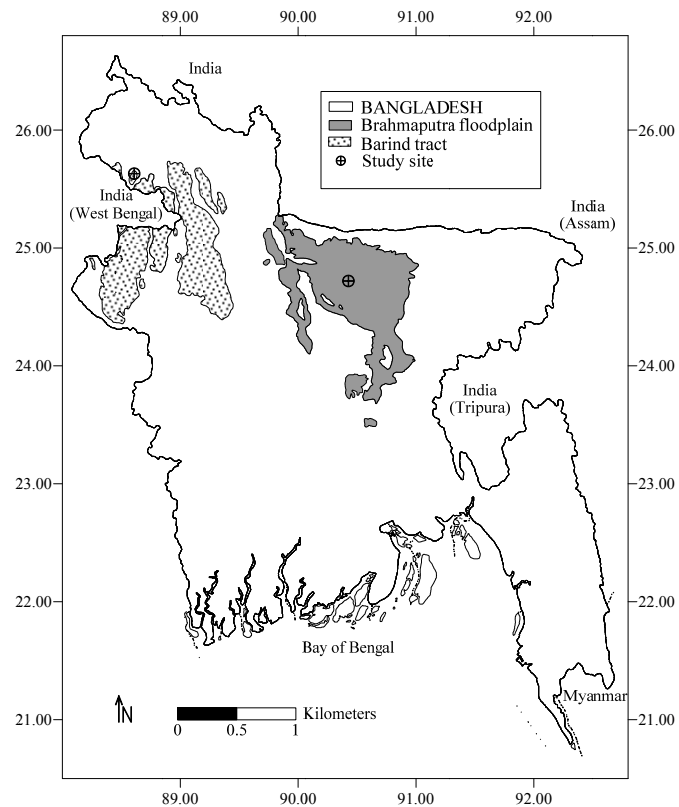


Figure 6. Location of the terrace (Barind Tract) and floodplain site in the map of Bangladesh

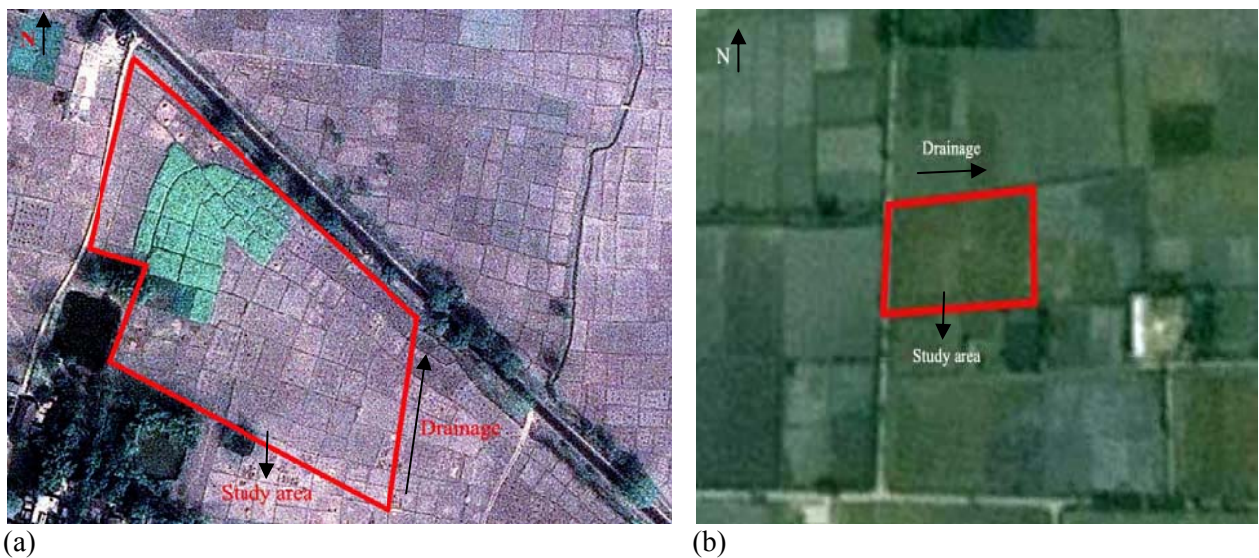


Figure 7. The location of (a) terrace study area (2.02 ha), (b) floodplain study area (0.8 ha), google earth image, dated: 31 January 2010

## **3.2 Terrace site**

### **3.2.1 Geology of the terrace soils of Bangladesh**

The terrace soils (commonly known as Barind Tract (BT)) are in the Pleistocene physiographic unit which occupies a nearly level to gently undulating landscape. This is mostly made up of older alluvium which differs from the surrounding floodplain. It comprises of three major sub-units: level, high and north-eastern BT. BT is floored by Pleistocene sediments which is compact and sticky known as the Madhupur Clay (MC). This semi-consolidated substratum is variably weathered, brown or yellowish brown in colour, deeply oxidised and assumed to be of fluvial origin and deposited towards the end of the last glacial period. Major part of this tract is poorly drained, mottled silty top soils merged with MC at shallower depth. The BT is fragmented, being made up separate uplifted fault blocks in the north eastern part of the country. It covers a total area of approximately 7,770 km<sup>2</sup> (Brammer, 2002 and 1996; Ibrahim and Baset, 1973).

### **3.2.2 Hydrology of BT**

The BT is bounded by three rivers: the Karatoya to the east, the Mahananda to the west and northern bank of the Ganges to the south but at present natural water flows have remarkably decreased causing several river affluents to be nearly extinct in the region. The contours of the BT suggest that there are two terrace levels: 40 m and the other between 19.8 - 22.9 m. About 47 % of the BT region is classified as high land, about 41 % as medium high land and the rest are low land. Most soils are shallowly flooded by rainwater within field bunds or by the raised ground water table in the rainy season (Brammer, 1996; Rashid, 1991).

### **3.2.3 Soil of BT**

The soil is imperfectly to poorly drained developed in shallowly weathered MC in level areas of the BT. The top soil is silty and light grey, generally brightly oxidised with yellowish brown mottles along cracks and root channels, and bears low level of organic matter. The soil belongs to Amnura soil series and subgroup - Aeric Haplaquept and order - Inceptisols in the USDA *Soil Taxonomy*. The cultivated layer is puddle and reduced in the monsoon season and under irrigated rice in the dry season. The soil becomes white and powdery when dry. The reaction is medium or strongly acidic when dry but the surface layer becomes neutral in reduced condition. The subsoil has a mixed yellowish brown and grey, red mottled, silty loam or silty clay loam texture which is commonly friable and porous. The soil shows a pronounced increase in mottles and clay content with depth. The substratum is strongly structured and compacted heavy plastic clay. The soil bears low natural fertility and has low moisture holding capacity. The low structural stability of the top soil and presence of a ploughpan which is beneficial for transplanted paddy but providing severe limitations for dry land crops (Brammer, 2002 and 1996; Ibrahim and Baset, 1973).

### **3.2.4 Climate of BT**

The BT lies in the monsoon region of the summer dominant hemisphere, generally it is rather hot and considered as semi-arid. The tropic of cancer lies south of this region. The climate of the area is generally warm and humid. Rainfall is comparatively little in this region, mean annual varies from 1500-1750 mm which is rather low compared to other parts of the country. It mainly occurs during the monsoon, rainfall varies from place to place as well as year to year. This region has already been designated as drought prone and suffering from scarcity of vegetation. Its average temperature ranges from 35 °C to 25 °C in the hottest season and 9 °C to 15 °C in the coolest season. In summer, some of the hottest days experience a temperature of about 45° C or even more and in winter, it falls to about 5 -10 °C in some places. The BT experiences extremes that are clearly in contrast to the climatic condition of the rest of the country (Brammer, 2002 and 1996; USG-Birol, 2008).

### **3.2.5 Electromagnetic induction (EMI) survey**

The soil conductivity sensor used in this research was the EM38 which is a non-invasive proximal soil sensor. The ECa survey was conducted July 25, 2009 and point measurements were taken in grid spacing of 17 by 10 m from a wet field. The calibration was done according to the steps described in the EM38 Operating Manual. ECa data in  $\text{mS m}^{-1}$  were recorded on a laptop computer. The EM38 was operated in both measurement modes, i.e., horizontal orientation (ECa-H) and vertical orientation (ECa-V). All the measurements were duly geo-referenced with a highly sensitive GPS manufactured by Navilock<sup>®</sup>. ECa data are expressed at 25 °C (Sheets and Hendrix, 2005), during the ECa measurements soil temperature was recorded at 20 cm depth using a soil thermometer. As the temperature of the soil was stable at 25.3 °C, no temperature correction of ECa data was required at the terrace site.

### **3.2.6 Soil sampling design**

The field was sampled according to a grid sampling design at 104 locations on a 17 by 10 m grid basis from a representative area of 2.02 ha. Composite soil samples were collected from a radius of 1 m. Soil samples were taken at three depth increments (0-30 cm, 30-60 cm and 60-90 cm) through augering from the marked geo-referenced locations the week following the ECa survey. The samples were analyzed by the Central laboratory, Soil Resource Development Institute (SRDI), Bangladesh.

### **3.2.7 Soil physical and chemical analysis**

#### **Particle size distribution**

Texture was determined by Hydrometer method described by Day, 1965. Calgon solution sodium hexametaphosphate) was used for dispersion. The densities of soil suspension were measured after various times, hence the particle size distribution was calculated. The following USDA size fractions were determined: Sand ( $>50\ \mu\text{m}$ ), Silt ( $2\text{-}50\ \mu\text{m}$ ) and Clay ( $<2\ \mu\text{m}$ ).

#### **Soil reaction**

The pH was determined by a glass-electrode pH meter in the soil suspension having a soil: water ratio of 1:2.5, after 30 minutes of shaking.

#### **Organic matter (OM)**

Dry combustion method (Loss on Ignition-LOI) was used for determination of organic matter. After oven drying (24 h at  $105\ ^\circ\text{C}$ ) of the sample to a constant weight organic matter is combusted to ash and carbon dioxide at a temperature between  $500\text{ - }550^\circ\text{C}$ . All organic matter is supposed to be volatilized as  $\text{H}_2\text{O}$  and  $\text{CO}_2$ . The weight loss corresponds to organic matter content of the soil.

#### **Total Nitrogen (N)**

Total nitrogen content of soils was determined by the Kjeldahl digestion method. Catalyst mixture ( $\text{K}_2\text{SO}_4$ :  $\text{CuSO}_4 \cdot 5\text{H}_2\text{O}$ : Se = 10: 1: 0.1), 30%  $\text{H}_2\text{O}_2$  and conc.  $\text{H}_2\text{SO}_4$  were used for digesting the soil samples. Nitrogen was estimated by distillation with 40% NaOH followed by titration of distillate trapped in  $\text{H}_3\text{BO}_3$  with 0.01 N  $\text{H}_2\text{SO}_4$ .

#### **Phosphorus (P)**

The available P content was determined by the Bray and Kurtz (1945) method using extractant HCL and  $\text{NH}_4\text{F}$ , and worked by dissolving Al-P and Fe-P minerals that control phosphate concentrations in acidic soils.

#### **Cation exchange capacity (CEC)**

After saturation with  $\text{BaCl}_2\text{-TEA}$  and one washing with water, the soil was shaken with a known amount of  $\text{MgSO}_4$  and centrifuged. The remaining Mg in an aliquot of the supernatant liquid was titrated with EDTA using ericchrome black-T indicator, and subtracted from a blank determination for calculation of CEC (Hendershot and Duquette, 1986).

## **Potassium (K<sup>+</sup>), Calcium (Ca<sup>2+</sup>) and Magnesium (Mg<sup>2+</sup>)**

The ammonium acetate (NH<sub>4</sub>OAc) extract method was used, which extracts the water soluble and rapidly exchangeable fractions of the alkaline earth cations by displacement with NH<sub>4</sub><sup>+</sup> from the exchange sites. This is done by the soil with a solution of 1 M NH<sub>4</sub>OAc adjusted to pH 7.0. After filtration, the amounts of K determined by flame emission, and Ca<sup>2+</sup> and Mg<sup>2+</sup> by atomic absorption spectroscopy (AAS) (Knudsen et. al., 1982).

### **Base saturation**

The base saturation refers to the relative number (percentage) of the CEC sites on the soil colloids that are occupied by bases such as Calcium (Ca<sup>2+</sup>), Magnesium (Mg<sup>2+</sup>), Potassium (K<sup>+</sup>) and calculated as,

$$\% \text{ Base saturation} = [(Ca^{2+} + Mg^{2+} + K^+)/CEC] * 100$$

### **3.2.8 Statistical and Geostatistical analysis**

The data analyses were conducted in three stages: i) Distribution was analyzed by classical statistics (mean, median, maximum, minimum, variance, standard deviation, skewness, kurtosis and coefficient of variation, frequency from histograms and scatter plots). Skewness is considered as the most common form of departure from normality. The exploratory statistical analyses were performed by PASW 18.0 (Predictive Analytics SoftWare) Statistics, ii) to find out the spatial structure of the selected soil properties, variography was used, variograms were calculated and modelled with VARIOWIN 2.2 software (Pannatier, 1996) and iii) the kriged maps of spatial distribution of selected soil properties were constructed using SURFER Version 9.2 software (Golden Software, Inc.). Ordinary kriging was used throughout.

#### **3.2.8.1 Spatial variation through variography**

Geostatistics view soil properties as continuous variables and models these as realizations of a random function or a random process (Webster, 2001). To characterize a random function assumptions are limited to the intrinsic hypothesis. The intrinsic hypothesis assumes stationarity of the first- and second-order moments of the increments  $[Z(x+h)-Z(x)]$  of the random function, where  $x$  is the location vector and  $h$  is a spatial lag. This implied that the expected value of the increments  $[Z(x+h)-Z(x)]$  is zero and their variance exists and both are independent of the position  $x$ . The two conditions are expressed as follows:

$$[Z(x+h)-Z(x)] = 0 \quad \forall x$$

$$\text{Var } [Z(x+h)-Z(x)] = E [(Z(x+h)-Z(x))^2] = 2 \gamma (h) \quad \forall x$$

Where,  $\gamma(h)$  is the semivariance, mostly called the (semi) variogram.

The semivariance measures the average dissimilarity between data separated by vector  $h$  and can be calculated based on a series of observations  $z(x_\alpha)$  (Goovaerts, 1997):

$$\gamma(h) = \frac{1}{2N(h)} \sum_{\alpha=1}^{N(h)} [z(x_\alpha + h) - z(x_\alpha)]^2$$

Where,  $\gamma(h)$  is the calculated semivariance for a lag vector  $h$  between observations  $z(x_\alpha)$  and  $z(x_\alpha+h)$  and  $N(h)$  the number of pairs of observations separated by  $h$ .

Ideally pairs of observations close together should have a smaller semi-variance, whereas pairs of observations farther away from each other should display a large semi-variance. A plot of the calculated  $\gamma(h)$  versus  $h$  yields the experimental variograms to which a theoretical model is fitted. Four of the most common variograms models are the spherical, the exponential, the gaussian and the linear model (Burrough, 1993). Unlike the first three model types, the linear model describes an unbounded variogram meaning that the variograms increases with increasing lag distance. Bounded variograms are characterized by three parameters which describe the spatial variance across the study area: the nugget variance ( $C_0$ ), the sill variance ( $C_0+ C_1$ ) and the range ( $r$ ). In theory, the semi-variance at  $h = 0$  is zero, but it is often found as the lag distance approaches zero, the semi-variance remains a positive value, called the nugget. The nugget is the intercept of the variogram with the Y-axis and represents unexplained spatiality dependent variation (micro variability at distances closer than the smallest sampling lag) or purely random variance (like measurement or sample error). The semi-variance increases with increasing lag until it stabilizes to a maximum, the still variance. The lag distance at which the still is reached is called the range. The still is the a priori sample variance  $\sigma^2$  and the range represents the limit of the spatial dependence since at that distance the autocorrelation become zero. Beyond the range, the expected difference between two observations is maximum (equalling the sill) and independent of the lag distance between them. At distances smaller than the range there exist a spatial dependence between two observations which increases with an increasing lag distance. So the variograms describes the pattern of spatial variability in terms of its magnitude, scale and general form (Oliver, 1987).

### 3.2.8.2 Spatial prediction through Kriging

Kriging is a geostatistical tool for the prediction of the value of a variable at an unsampled location on the basis of sample observations made in its neighbourhood. It is a weighted linear estimator where the weights are derived using the variogram ensuring an unbiased estimation with a minimum estimation error (Webster and Oliver, 1990). Kriging provides a Best Linear Unbiased Estimator (BLUE) (Burrough and McDonnel, 1998). A variety of Kriging algorithms

are available, such as ordinary and simple Kriging use the target (primary) variable to make predictions. On the other hand, techniques such as co-kriging use the joint spatial variation of the target variables and densely measured ancillary variables, such as ECa, to improve the prediction accuracy. In this dissertation, ordinary Kriging was used as a common methodology for the prediction of soil variables. The probabilistic interpolators aim to give optimal representation of the stochastic part of the regionalized variable, the local interpolator is extended to a more geostatistical form giving general Kriging equation.

Consider a random variable  $Z$  that has been measured at  $n$  locations,  $z(x_\alpha)$ ,  $\alpha = 1, \dots, n$ , the Kriging estimator at an unsampled location  $x_0$  can be written as:

$$Z^*(x_0) - m(x_0) = \sum_{\alpha=1}^{n(x_0)} \lambda_\alpha \cdot [z(x_\alpha) - m(x_\alpha)]$$

Where  $n(x_\alpha)$  is the number of neighbourhood measurements  $Z(x_\alpha)$  used for estimating  $Z^*(x_0)$ ,  $\lambda_\alpha$  are the weights assigned to data  $Z(x_\alpha)$  which are considered to be a realization of the random variable  $Z$ , and  $m(x_0)$  and  $m(x_\alpha)$  are the expected values (or means) of  $Z^*(x_0)$  and  $Z(x_\alpha)$ , respectively. The weights are calculated minimizing the estimation error variance:

$$s^2(x_0) = E \{ [Z^*(x_0) - Z(x_0)]^2 \}$$

Under the condition of unbiasedness:

$$E [Z^*(x_0) - Z(x_0)] = 0$$

### 3.2.8.3 Ordinary Kriging (OK)

Ordinary Kriging is the most common type of Kriging used in geostatistics and it serves to estimate a value at a point of a region for which a variogram is known using data in the neighbourhood of the estimation location. However it assumes the mean of the observations to be unknown but locally stationary. The ordinary Kriging estimator  $Z^*(x_0)$  can be written as:

$$Z^*(x_0) = \sum_{\alpha=1}^{n(x_0)} \lambda_\alpha Z(x_\alpha) = 1 \quad \text{with} \quad \sum_{\alpha=1}^{n(x_0)} \lambda_\alpha = 1$$

Where  $n(x_0)$  is the number of observations in the local neighbourhood around  $x_0$  and  $\lambda_i$  are the weights assigned to each of these observations which results the expected interpolation.

### **3.3 Floodplain site**

#### **3.3.1 Geology of the floodplain soils of Bangladesh**

The floodplain is formed by deposits and sediments associated with different rivers of the country. Most of the fertile cultivable lands belong to floodplain which is unconsolidated sediments occupying about 80 % of the country. These sediments are far from being homogenous in age, texture or mineralogy. They have been deposited under different geomorphological conditions in different areas: piedmont plains near the foot of hill (the Himalayas), river meander floodplains, estuarine floodplain and tidal floodplain. New alluvium is still being deposited near to river channels but most floodplain land has received little or no new alluvium for several hundred years or more. Rivers has changed their courses from time to time in the past and thus providing sediments of different ages in different places. The floodplain sediments have high silt content. The study site belongs to meander floodplain soil commonly known as old Brahmaputra floodplain (BF). This soil mostly overlies a sandy substratum at moderately shallow depth. The BF is the second most extensive soils in the comprising 1,599,645 ha which is 13 % of the total floodplain area. This old floodplains is virtually stable land as the main river channel has moved away but they are crossed by tributary or distributaries channels (Brammer, 2002 and 1996).

#### **3.3.2 Soil of BF**

The soil is imperfectly to poorly drained, seasonally flooded and the flooding is predominantly through within field bunds or ponded monsoon rainwater. It belongs to Sonatola soil series comprises of non calcareous dark grey soil consisting of mostly medium high land. The soil series belongs to subgroup - Aeric Haplaquept and order - Inceptisol in the USDA *Soil Taxonomy*. The puddled top soil has been cultivated for transplanted rice and overlying a ploughpan. Topsoil is slightly acidic in reaction when not submerged. The subsoil is grey and or dark grey or has prominent grey coatings on the faces of subsoil cracks and pores. The topsoil has silt loam and silt clay loam in texture while sub- and deepsoil has silt loam texture. The original alluvial stratification within 30 cm from the surface has been broken up by biological mixing, the subsoil has developed structure and oxidised mottles (Brammer, 2002 and 1996).

#### **3.3.3 Hydrology of BF**

The country's topography, geology and hydrology are mainly influenced by the three major rivers Ganges, Brahmaputra and Meghna, and their associated affluents, river branches and connecting channels. A remarkable change in the course of the Brahmaputra river took place 200 years ago, the river shifted from its course. The new portion of the Brahmaputra is named as the Jamuna river. The old course shrank through silting into a small seasonal channel only two kilometres broad and built up fair high levees on either side over which the present river rarely spills the generally smooth landscape of broad ridges and basin. This old floodplain exhibits a

gentle morphology composed of broad ridges which are subject to shallow flooding only in the monsoon through ponded rainwater, and accumulation of local runoff and the raised ground water table (Brammer, 2002 and 1996).

### 3.3.4 Climate of BF

Three main seasons are generally recognized in the country. A hot, humid summer from March to June; a cool, rainy monsoon season from June to October; and a cool, dry winter from October to March. In general, maximum summer temperatures range between 32 °C - 38 °C. April is the warmest month in most parts of the country. January is the coldest month, when the average temperature for most of the country is 10 °C. Heavy rainfall is characteristic of Bangladesh with the exception in the BT region. About 80 percent of Bangladesh's rain falls during the June to October monsoon season with a mean annual average of 2275 mm (USG-Mymensingh sadar, 2009).

### 3.3.5 Electromagnetic induction (EMI) survey

The EM38 sensor was housed into a Floating Soil Sensing System (FloSSy) which was designed and prepared by Islam (2009) of ORBit research group. The FloSSy consists of an EMI soil sensing instrument (EM38), a GPS, a field laptop, a real time sensor data processing and path guidance software, the GPS and vehicle to pull the entire sensing platform (Figure 8). The features of the FloSSy are provided in Appendix 11.



Figure 8. Floating Mobile Soil Sensing System during field measurement of ECa; close up views show individually labeled components of the system (Islam, 2009)

The ECa measurements were obtained continuously as 4 readings per seconds, i.e., 1 m width (distance in-between adjacent lines) x 25 cm length (distance along a line and 1 measurement point represent 1 m<sup>2</sup> of the field (Appendix III). The continuous ECa measurement was done in

two orientations and the field was in dry condition. The measured EC<sub>a</sub> data were converted to EC<sub>a</sub> at 25 °C, as soil temperature was recorded 29 °C, using the following equation (Sheets and Hendrix, 1995):

$$EC_{25} = EC_a(0.4470 + 1.4034e^{-\frac{T}{26.815}})$$

Where, EC<sub>25</sub> = Electrical conductivity at the reference temperature of 25 °C

T = Soil temperature in degrees Celsius

### **3.3.6 Soil sampling design**

The field was sampled according to a grid sampling design at 20 locations on a 20 by 17 m grid basis from a representative area of 0.8 ha. Soil samples were taken at three depth increments (0-30 cm, 30-60 cm and 60-90 cm) through augering from geo-referenced locations the week following the EC<sub>a</sub> survey. The samples were sent to Soil Testing Laboratory, Soil Science Department, Bangladesh Agricultural University, Bangladesh and Soil Science Laboratory at Department of Soil Management of Ghent University, Belgium.

### **3.3.7 Soil physical and chemical analysis**

#### **Particle size distribution**

Soil textural analysis was performed using the pipette method following the procedure described by Gee and Bauder (1986). Twenty grams of air dried soil was treated with HCl (37 %) to destroy carbonates. Subsequently, the organic materials were destroyed by heating the soil sample with H<sub>2</sub>O<sub>2</sub> (30 %) at 70 °C until the reaction stops. The sample was heated to evaporate H<sub>2</sub>O<sub>2</sub> and then washed with distilled water for three times to remove the excess HCl. Afterwards, a mixture of sodium hexametaphosphate ((NaPO<sub>3</sub>)<sub>6</sub>) and sodium carbonate (Na<sub>2</sub>CO<sub>3</sub>) was added to disperse the soil particles. The sand fraction was separated by wet sieving through a 50 µm sieve and weighed after oven drying. The remaining clay and silt fractions (0 to 50 µm) were taken into a one-litre volumetric cylinder and distilled water used to volume. Immediately after thoroughly shaking the soil solution, a suspended sample consisting of silt and clay fraction was pipetted out at room temperature and oven dry weight was determined. A sample of clay in the soil suspension was pipetted out after allowing the silt fraction to settle for 6 hrs 47 minutes at 25 °C. The oven dry weight of the clay fraction in the pipetted sample was determined. The silt content was calculated by subtracting the weight of clay fraction from the dry weight of the firstly pipetted sample. Subsequently, the percentage sand, silt and clay fraction were calculated.

## **Organic C**

The organic C content was determined by the Walkley and Black method described by Nelson and Sommers (1996). One gram of soil sample was treated with potassium dichromate ( $K_2Cr_2O_7$ ) and  $H_2SO_4$ , in order to oxidize the organic matter. Upon completion of the oxidation phase, the unused or excess dichromate ions ( $Cr_2O_7^{-2}$ ) were determined to obtain the organic C content. Therefore, the digestate was back titrated with ferrous sulphate ( $FeSO_4$ ). The calcium carbonate content was obtained by treating one gram of soil with  $H_2SO_4$ , and subsequent back titration of the unused  $H_2SO_4$  with NaOH.

## **Total Nitrogen (N) and soil reaction**

Referred to section 3.2.7

## **Cation exchange capacity (CEC)**

Cation exchange capacity of soil was determined by saturating the soil samples with NaOAc and replacing  $Na^+$  from the saturated sample by 1N  $NH_4OAc$  (pH 7.0). Sodium in the solution was then determined by Flame Photometer at 589 nm wavelength (Chapman, 1965).

## **Exchangeable Calcium ( $Ca^{2+}$ ) and Potassium ( $K^+$ )**

Exchangeable  $K^+$  and  $Ca^{2+}$  contents of soil were determined by atomic absorption spectrophotometer after extraction with 1N  $NH_4OAc$  at pH 7.0.

## **Electrical conductivity (ECe)**

Electrical conductivity (ECe) of aqueous soil extracts was obtained from 1:5 soils to water mixture by vacuum filtration, and measured by filling and EC electrode with soil extract using 0.01N KCl solution to calibrate the meter (Biswas and Mukherijee, 1987).

## **3.3.8 Statistical and Geostatistical analysis**

Referred to section 3.2.8

## 4. Results and Discussion

This part describes the results of the exploratory and geostatistical data analysis of the observed physical and chemical soil properties. The objective was to configure the nature and extent of within-field variability of the two study sites through soil mapping. For this purpose, geo-referenced ECa measurements were taken including a total of 312 soil samples in the terrace site and 60 samples in the floodplain site. The spatial variability of the soil properties were discussed according to topsoil (0-30 cm), subsoil (30-60 cm) and deepsoil (60-90 cm) characteristics.

### 4.1 Terrace site

#### 4.1.1 Descriptive statistics

##### 4.1.1.1 Soil properties

The soil properties were approximately of symmetrical distribution. This was further confirmed by their respective coefficients of skewness (Table 1 and 2). The frequency distribution of the selected soil properties are shown in figure 9 and 10.

The mean particle size distribution of the topsoil corresponded to silt loam texture class while subsoil textural distributions were clay loam, silty clay and silty clay loam. The deepsoil clearly corresponded to clay texture class. The coefficient of variation (CV) of textural fractions (9 - 47 %) showed considerable variation which was relatively high for sand fraction. The topsoil texture fractions showed large variability in comparison to subsoil and deepsoil which was reflected by their respective CV's (Table 1). However, the textural data were superimposed on the USDA texture triangle (Figure 11) which indicated that more than 90 % of the observations for the topsoil classified into silt loam, 70 % of the subsoil into clay loam and the rest belongs to silty clay and silty clay loam texture class. For the deepsoil, the majority of the observations corresponded to clay texture class.

The examined chemical properties showed larger within-field variability for all the properties except total N which was further explained by their relatively higher CV's (Table 2). Soil in the terrace site featured a high level of acidity (mean pH 5.07) and low level of organic C (mean 8.45 g kg<sup>-1</sup>) which varied greatly from 3.90 to 18.26 g kg<sup>-1</sup>. A medium level of CEC (mean 12.63 cmol<sup>+</sup> kg<sup>-1</sup>) was found. The percentage of base saturation in the investigated site varied from 23 to 43 % with a mean of 32 %. The total N was found to be low and available P was in an optimum level. The level of exchangeable cation, Ca<sup>2+</sup> was observed to be medium while the level of Mg<sup>2+</sup> and K<sup>+</sup> were low. The levels of chemical property were determined according to Fertilizer Recommendation Guide (2005). The critical limits are shown in appendix IV.

Table 1. Descriptive statistics of textural fractions in the terrace site, n = 104

<b>Top soil (0-30 cm)</b>									
Variable	Mean	Median	Min	Max	Variance	Std. dev.	Skewness	Kurtosis	CV (%)
Clay	23	23	15	29	13.95	3.74	-0.28	-0.98	16
Silt	60	60	49	70	30.29	5.50	0.00	-1.16	9
Sand	17	17	4	35	64.36	8.02	0.15	-1.11	47
<b>Subsoil (30-60 cm)</b>									
Clay	38	38	32	45	12.24	3.50	0.13	-1.27	9
Silt	40	30	32	47	11.88	3.45	0.20	-0.63	9
Sand	22	24	9	36	42.44	6.51	-0.27	-0.10	30
<b>Deepsoil (60-90 cm)</b>									
Clay	43	44	34	55	21.27	4.61	0.00	-0.64	11
Silt	31	40	22	37	10.86	3.30	-0.23	-0.31	11
Sand	26	27	12	39	42.83	6.54	0.04	-0.96	25

Table 2. Descriptive statistics of topsoil chemical properties in the terrace site, n = 104

Variable	Units	Mean	Median	Min	Max	Variance	Std. dev.	Skewness	Kurtosis	CV (%)
pH water		5.07	5.00	4.30	6.20	0.19	0.44	0.33	-0.90	9
Organic C	g kg <sup>-1</sup>	8.45	7.67	3.90	18.26	7.89	2.81	1.33	1.88	33
Total N	g kg <sup>-1</sup>	1.16	1.20	0.30	2.30	0.23	0.48	0.03	-0.86	4
Avil. P	mg kg <sup>-1</sup>	19.43	19.97	11.67	26.94	11.37	3.37	0.23	-0.59	17
CEC	cmol <sup>+</sup> kg <sup>-1</sup>	12.63	12.50	8.50	17.30	4.02	2.00	0.37	-0.60	16
Ca <sup>2+</sup>	cmol <sup>+</sup> kg <sup>-1</sup>	3.10	2.93	2.11	4.74	0.32	0.57	0.64	-0.29	18
Mg <sup>2+</sup>	cmol <sup>+</sup> kg <sup>-1</sup>	0.83	0.84	0.21	1.32	0.07	0.26	-0.26	-0.76	31
K <sup>+</sup>	cmol <sup>+</sup> kg <sup>-1</sup>	0.14	0.13	0.07	0.31	0.00	0.04	1.35	3.04	29
Base saturation	%	32	32	23	43	13.54	3.68	0.27	0.47	12

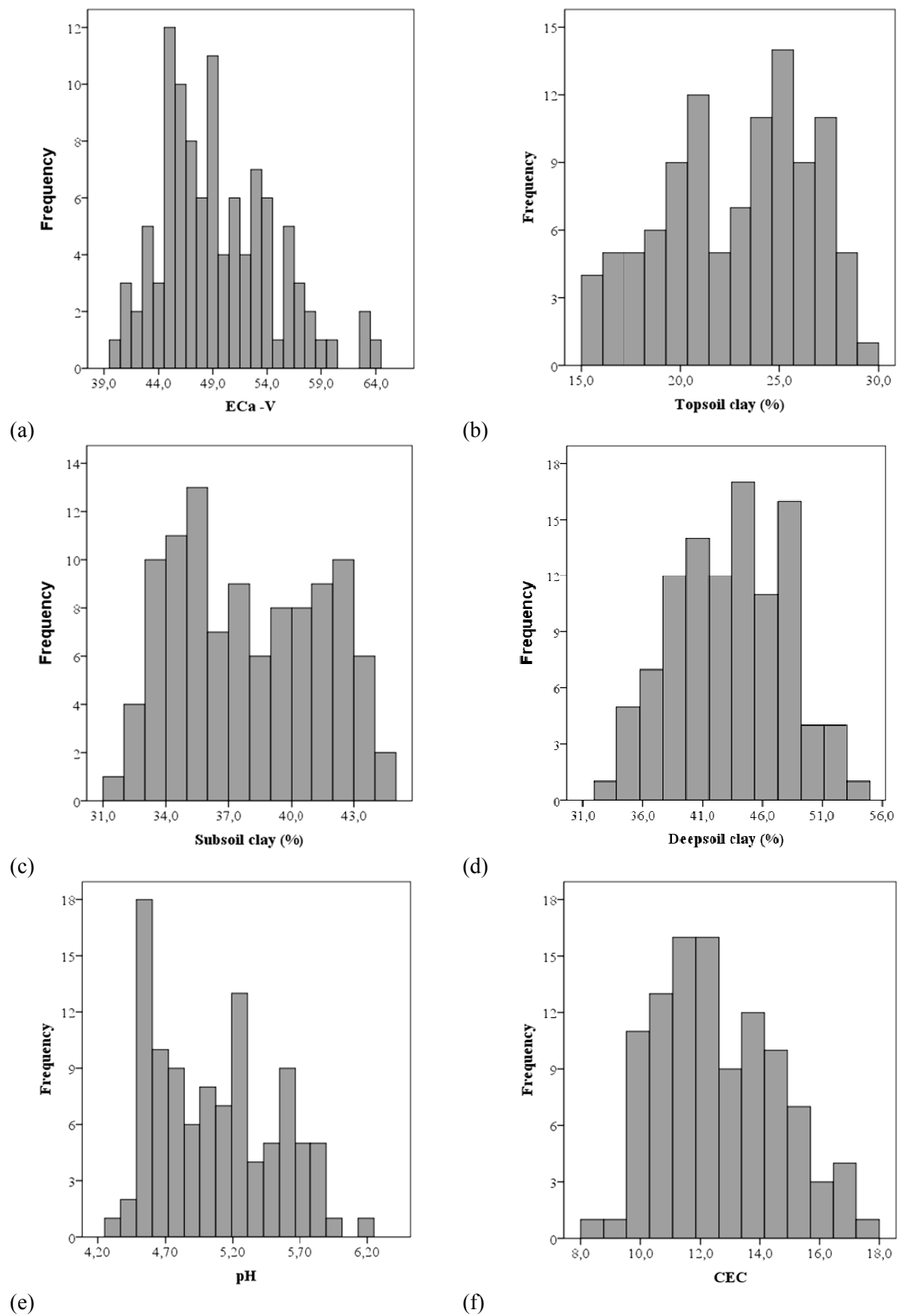


Figure 9. Histograms of a) ECa-V (mS m<sup>-1</sup>), b) topsoil clay, c) subsoil clay, d) deepsoil clay e) pH, and f) CEC (cmol<sup>+</sup> kg<sup>-1</sup>) in the terrace site

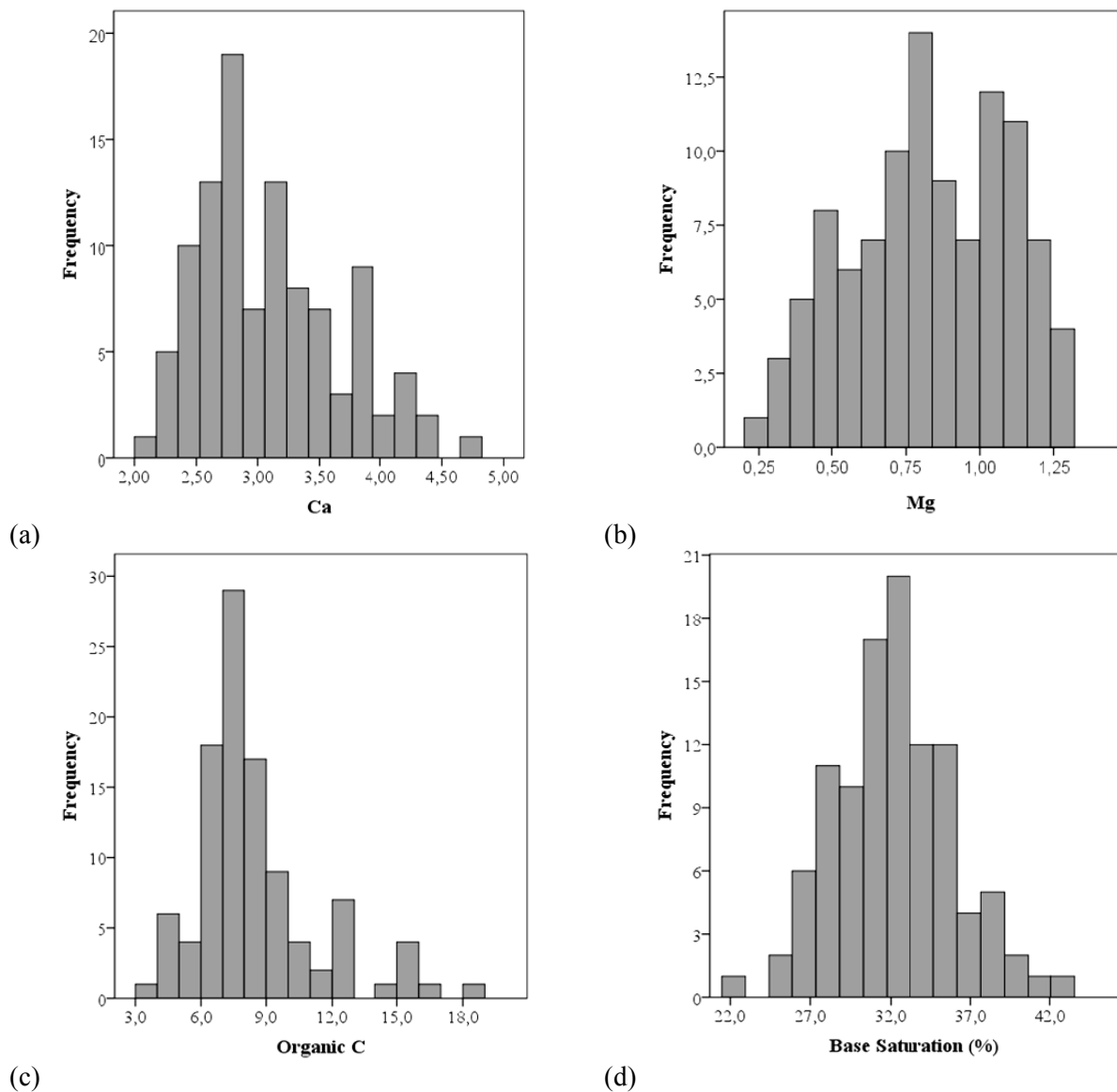


Figure 10. Histograms of a)  $\text{Ca}^{2+}$  ( $\text{cmol}^+ \text{kg}^{-1}$ ), b)  $\text{Mg}^{2+}$  ( $\text{cmol}^+ \text{kg}^{-1}$ ), c) Organic C ( $\text{g kg}^{-1}$ ) d) Base saturation (%) in the terrace site

#### 4.1.1.2 Apparent electrical conductivity (ECa)

The ECa measurements were approximately of symmetrical distribution and skewed to the right. The ECa readings ranged from 32 to 53  $\text{mS m}^{-1}$  and 40 to 64  $\text{mS m}^{-1}$  for the horizontal and vertical orientation of measurement respectively in the terrace site. The readings of ECa-V measurement were relatively larger than those of the simultaneous ECa-H (Table 3). The coefficients of variation (CV's) were in the same order in both orientations. The two orientations ECa measurement were well correlated with a linear positive correlation coefficient of  $r = 0.81$ .

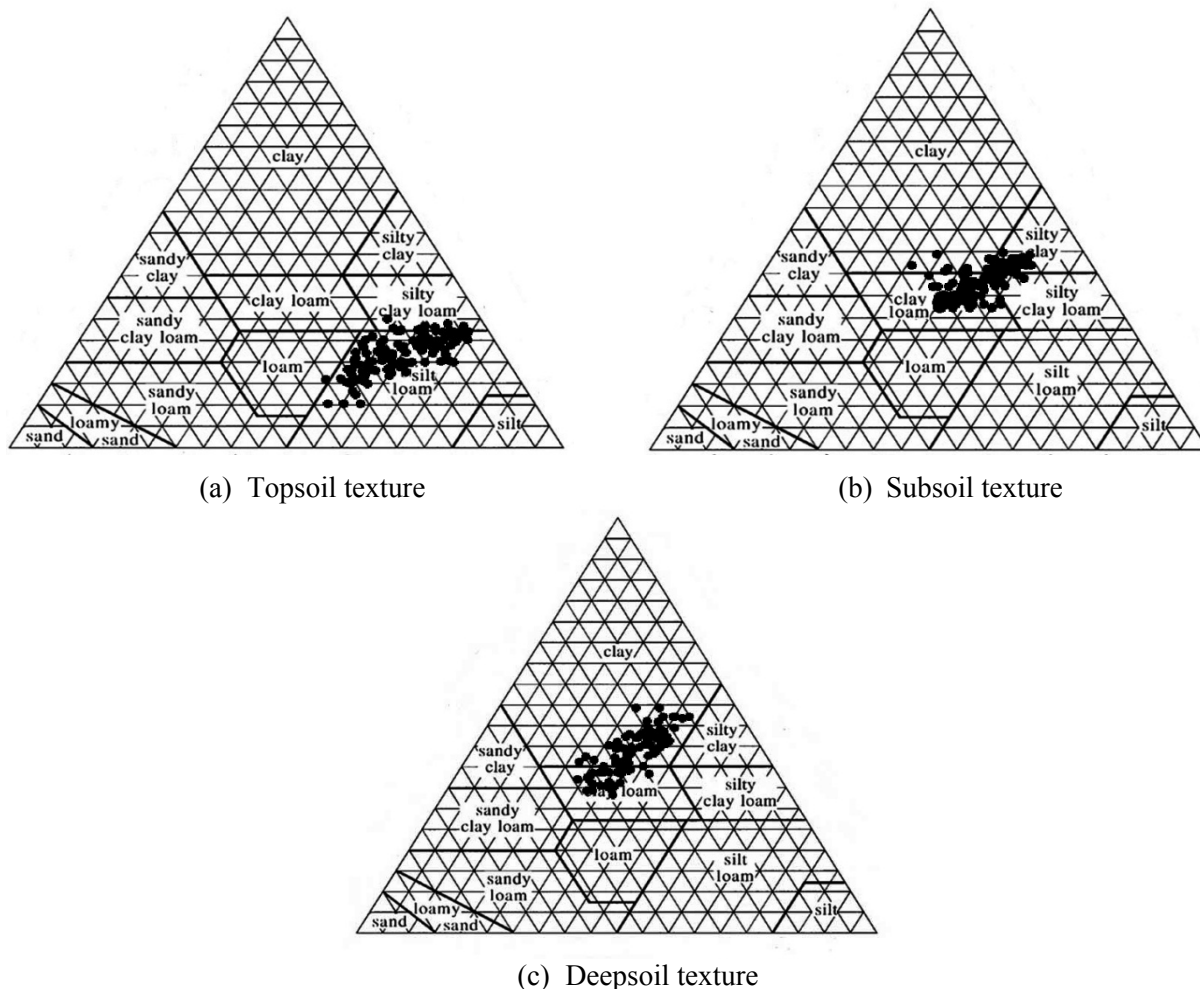


Figure 11. The distribution of a) topsoil, b) subsoil and c) despoil textural class in the USDA texture triangle in the terrace site

**Table 3. Descriptive statistics of ECa ( $\text{mS m}^{-1}$ ) measurements in the terrace site**

Variable	n	Mean	Median	Min	Max	Variance	Std. dev.	Skewness	Kurtosis	CV (%)
ECa-H	104	39.3	38	32	53	22.83	4.78	0.88	0.41	10
ECa-V	104	49.4	49	40	64	26.49	5.15	0.63	0.09	10

ECa-H and ECa-V, apparent ECa measured in the horizontal and vertical mode respectively

#### 4.1.2 Correlation coefficients of ECa with textural and chemical soil properties

##### 4.1.2.1 ECa and texture

Pearson product moment ( $r$ ) correlations were calculated between ECa and textural fractions, as shown in table 4. The scatter plots are shown in figure 12. The best positive linear correlation ( $r$

= 0.78) occurred between ECa-V and subsoil clay. The correlation between ECa-V and deepsoil ( $r = 0.68$ ) nearly coincided with subsoil clay while the correlation with topsoil clay was relatively lower ( $r = 0.57$ ). The negative correlation coefficients between ECa-V and the sand fractions were  $r = -0.60$ ,  $r = -0.84$  and  $r = -0.75$  for the top-, sub- and deepsoil sand respectively. These correlations were likely due to an evident increase of clay throughout the examined depth in the reference site. The weight of  $r$  values were corresponded with increasing clay and indicated the importance of clay content in determining soil ECa readings for non-saline soil (Kühn et. al., 2009; Triantafilis et. al., 2009; Bronson et. al., 2005). In addition, the spatial variation in the ECa readings is controlled mainly by clay content and mineralogy for soils in a humid climate containing negligible amounts of salts (Lesch et. al., 2005; Auerswald et. al., 2001). The similar trends of correlations were observed for ECa-H but the strength was relatively lower than the ECa-V, as shown in table 4. The kriged map of ECa-V more closely reflects the spatial distribution of subsoil and deepsoil clay than the ECa-H map. More specifically, the survey provides fairly representative soil ECa-V map of the spatial extent and magnitude of clay and sand content of the reference site. Furthermore, the EM38 readings measured in the vertical dipole mode were more predictive than the horizontal dipole mode readings.

Table 4. Pearson correlations ( $r$ ) of ECa and textural fractions in the terrace site,  $n = 104$

	ECa-V	ECa-H	T_clay	S_clay	D_clay	T_silt	S_silt	D_silt	T_sand	S_sand	D_sand
ECa-V	1	0.81**	0.57**	0.78**	0.68**	0.47**	0.66**	0.45**	-0.60**	-0.84**	-0.75**
ECa-H		1	0.50**	0.60**	0.58**	0.28*	0.61**	0.44*	-0.43*	-0.70**	-0.65**
T_clay			1	0.62**	0.57**	0.50**	0.35*	0.25*	-0.80**	-0.56**	-0.53**
S_clay				1	0.63**	0.45*	0.56**	0.35**	-0.59**	-0.88**	-0.63**
D_clay					1	0.43*	0.50**	0.33**	-0.54**	-0.64**	-0.87**
T_silt						1	0.41*	0.36**	-0.92**	-0.49**	-0.49*
S_silt							1	0.43*	-0.45**	-0.87**	-0.57**
D_silt								1	-0.37*	-0.45*	-0.74**
T_sand									1	0.61**	0.58**
S_sand										1	0.69**
D_sand											1

ECa-H and ECa-V ( $\text{mS m}^{-1}$ ), apparent ECa measured in the horizontal and vertical mode respectively and  $P \leq 0.01$ \*\*,  $0.05$ \*.

#### 4.1.2.2 ECa and chemical properties

The association between ECa and the examined chemical properties were reflected by the Pearson product moment ( $r$ ) correlation coefficient as shown in table 5. The scatter plot between ECa-V and CEC is shown in figure 12d.

Table 5. Pearson correlations of ECa and topsoil chemical properties in the terrace site,  $n = 104$

Variable	ECa-V	ECa-H	OC	CEC	Ca <sup>2+</sup>	Mg <sup>2+</sup>	K <sup>+</sup>	BS	Total N	P	pH
ECa-V	1	0.81**	0.16	0.53**	0.51**	0.66**	-0.17	0.23*	-0.27**	-0.14	0.46**
ECa-H		1	0.03	0.43**	0.40**	0.50**	-0.27**	0.14	-0.34**	-0.18	0.36**
OC			1	0.64**	0.51**	0.33**	0.55**	-0.04	0.43**	-0.15	0.28**
CEC				1	0.76**	0.58**	0.23*	-0.12	0.02	-0.22*	0.45**
Ca <sup>2+</sup>					1	0.53**	0.19	0.48**	0.02	-0.24*	0.53**
Mg <sup>2+</sup>						1	0.08	0.42**	-0.12	-0.05	0.29**
K <sup>+</sup>							1	0.05	0.62**	0.03	0.14
BS								1	-0.03	-0.03	0.20*
Total N									1	0.18	0.04
P										1	-0.14
pH											1

ECa-H and ECa-V (mS m<sup>-1</sup>), apparent ECa measured in horizontal and vertical mode respectively; OC, % organic C; CEC (cmol<sup>+</sup> kg<sup>-1</sup>), cation exchange capacity; Exchangeable Ca<sup>2+</sup>, Mg<sup>2+</sup> and K<sup>+</sup> (cmol<sup>+</sup> kg<sup>-1</sup>); BS, % Base saturation; Total N (g kg<sup>-1</sup>); Available P (mg kg<sup>-1</sup>); pH water, 1 : 2.5 and  $P \leq 0.01^{**}, 0.05^{*}$ .

In the terrace site, positive linear correlation coefficients ( $r = 0.46$ ,  $r = 0.53$ ,  $r = 0.51$  and  $r = 0.66$ ) were found between ECa-V, and pH, CEC, Ca<sup>2+</sup> and Mg<sup>2+</sup> respectively. Corwin and Lesch (2005) reported pH, CEC and Mg<sup>2+</sup> to be related with ECa measurements while McBride et. al. (1990) and Triantafilis et. al. (2009) related ECa measurements to CEC, and exchangeable Ca<sup>2+</sup> and Mg<sup>2+</sup>. Furthermore, correlations of ECa with clay content and CEC were generally highest and most persistent. It may be feasible to develop relationships between ECa and clay, and CEC that are applicable across a wide range of soil and climatic conditions (Sudduth et. al., 2005). However, the correlation coefficients were relatively higher for ECa-V than the ECa-H in the reference site. The observed correlations suggest that ECa-based sample design will provide a better spatial representation for those four properties. The weakly correlated properties were organic C, K<sup>+</sup>, base saturation, total N and available P.

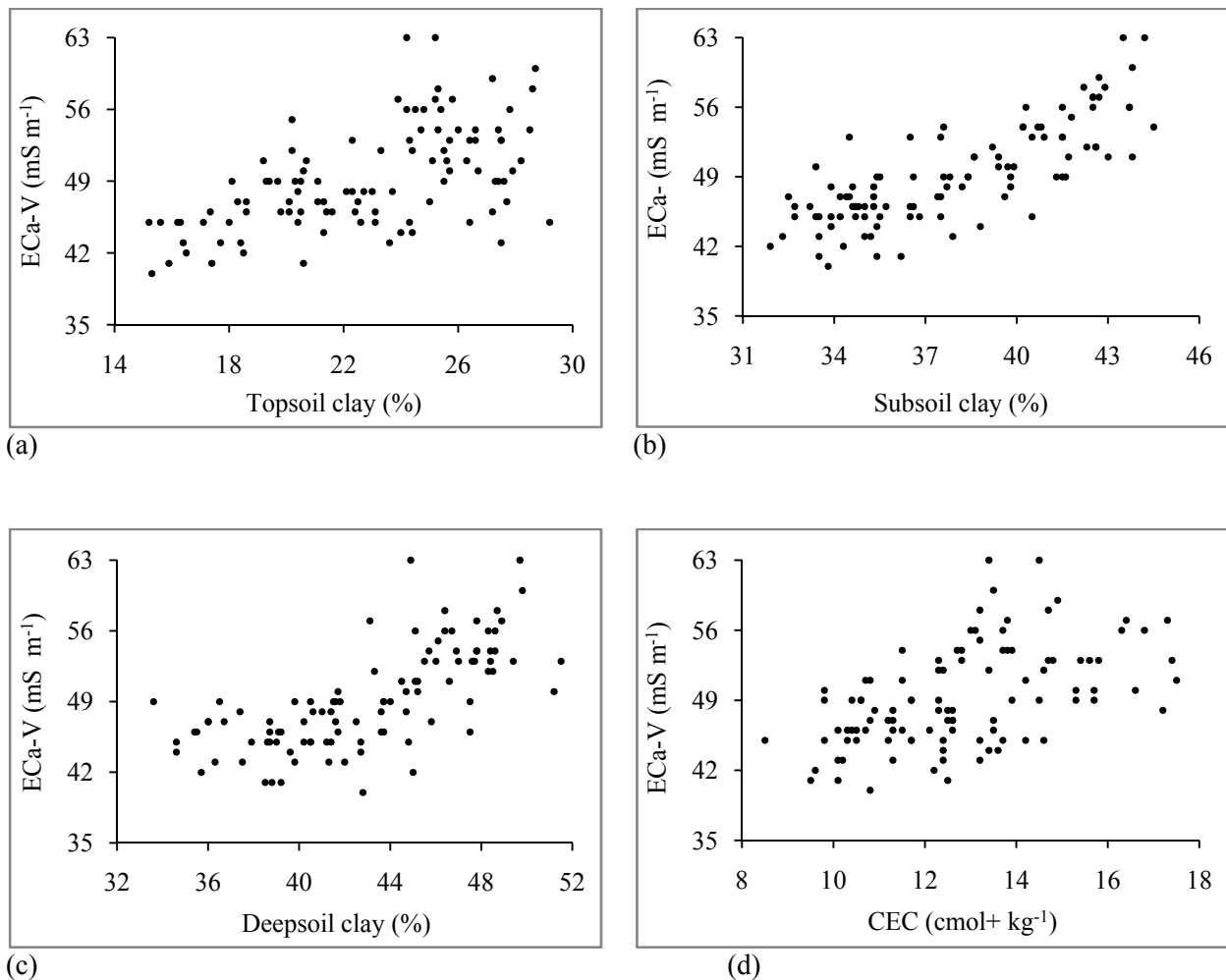


Figure 12. Scatter plots between ECa-V and a) topsoil, b) subsoil, c) deepsoil clay and d) CEC in the terrace site

### 4.1.3 Spatial variability of soil properties

#### 4.1.3.1 Mapping of ECa measurements

The horizontal and vertical ECa data sets were modeled with omni-directional spherical variograms (Figure 13). The model parameters were listed in table 6. The spatial variability of ECa showed ranges of 27 m and 30 m of approximate distance at which spatial autocorrelation between data points pairs ceases or becomes much more variable for ECa-H and ECa-V respectively. The relative nugget effects (RNE), i. e., the ratio of nugget variance to the total variance (the sill), were found nearly similar which indicated that spatial variability of ECa approximately highly structured by the fitted models. Furthermore, the variograms had a strong spatial structure as only 32 % and 30 % of the variability remain unaccountable or the variance not attributable to spatial dependence. However, the data sets were kriged to construct their continuous surface soil ECa maps (Figure 14 and 15) where the ordinary kriging interpolation technique was used. The map of ECa-H and ECa-V with grid geometry 1 by 1 m showed similar pattern and mutual integrity.

Table 6. Model parameters of the fitted omni-directional spherical variograms

Variogram parameters				
Variable	$C_0$ , nugget variance ( $\text{mSm}^{-1})^2$	$C$ , sill ( $\text{mSm}^{-1})^2$	$h$ , range (m)	RNE, relative nugget effect (%)
Eca-H	6.7	21.1	27	32
Eca-V	6.7	22.6	30	30

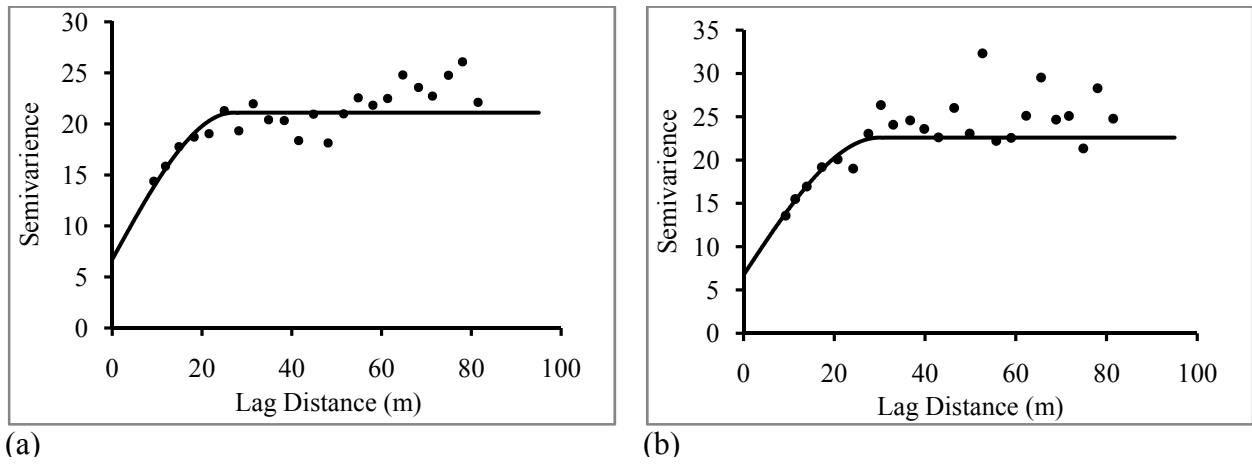


Figure 13. Variograms of a) Eca-H and b) Eca-V of the terrace site

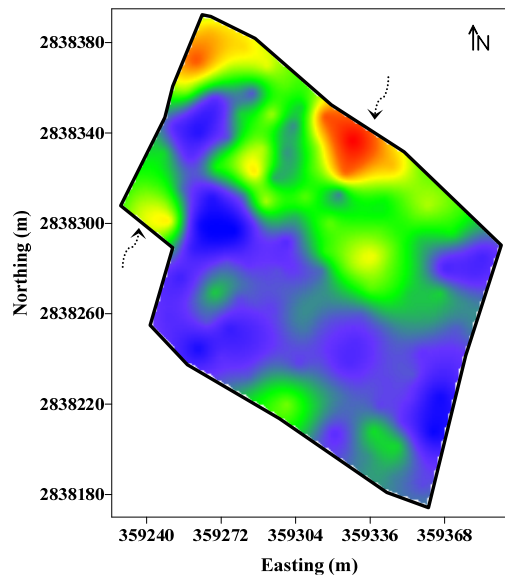


Figure 14. Interpolated values in  $\text{mS m}^{-1}$  for Eca-H in the terrace site.

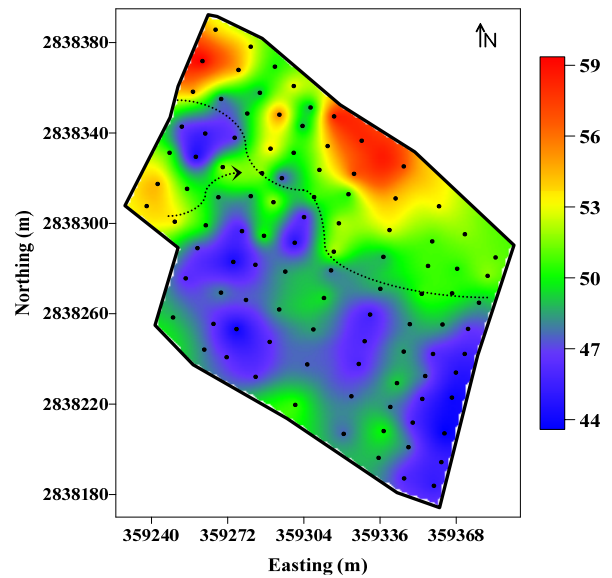


Figure 15. Interpolated values in  $\text{mS m}^{-1}$  for Eca-V with sampling locations (shown as dots) in the terrace site.

#### 4.1.3.2 Mapping of clay and sand content

The fitted spherical variograms for the clay and sand fractions are shown in figure 16 while the model parameters are listed in table 7.

Table 7. Model parameters of omni-directional spherical variograms for the textural fractions

Variogram parameters	Topsoil			Subsoil			Deepsoil		
	Clay	Silt	Sand	Clay	Silt	Sand	Clay	Silt	Sand
$C_0$ , nugget variance ( $\text{mS m}^{-1}$ ) <sup>2</sup>	2	13	16.7	5.8	4.5	15	7.3	5	22
$C$ , sill ( $\text{mS m}^{-1}$ ) <sup>2</sup>	11.8	29.4	58.1	11.8	10.9	35.1	20.3	10.5	43
$h$ , range (m)	30	30	35	42	18	30	32	42	42
RNE, relative nugget effect (%)	17	44	29	49	41	43	36	48	51

The fitted models suggest that the variability is well structured in space and is isotropic. The presence of nugget variance might be due to short range variability which mainly takes place at distances smaller than the sampling interval. The ratio of nugget variance to the sill variance can be considered as a criterion to specify the spatial dependence of the variables. Cambardella et. al. (1994) suggested that if the ratio of nugget to the sill (RNE) is lower than 25 %, spatial correlation is classified as high, 25 to 75 % as medium and over 75 % as low. The RNE of topsoil clay was 17 % which means clay possessed a strong spatial dependence while for sub- and deepsoil clay the spatial dependence is moderate, the RNE value is 49 % and 36 % respectively. The sand content is moderately spatially dependent which is further explained by the respective RNE's shown in table 7. On the other hand, the range of spatial dependence can be considered as the distance beyond which observations are not spatially correlated. The spatial dependence for topsoil and deepsoil clay is found at a nearly similar separation distance of 30 and 32 m respectively while the subsoil spatial autocorrelation become much weaker from 42 m apart. In case of sand distribution for each depths increment the approximate distance at which autocorrelation ceases were 35 m, 30 m and 42 m respectively.

The clay content sharply increases with depths in the terrace site. The mean clay contents were 23 %, 38 % and 43 % for the 0-30 cm, 30-60 cm and 60-90 cm depth increments respectively. The subsoil showed distinctly higher clay content than the overlying topsoil causing an abrupt textural change between top and subsoil. The subsoil clay content was nearly twice that of the topsoil, and even more in the deepsoil with a maximum around 50 %. This textural difference might be caused by an illuvial accumulation of clay or by pedogenetic formation of clay in the subsoil or destruction of clay in the surface horizon or by a combination of two or more of these processes. However, the kriged clay content maps showed that the topsoil and subsoil clay

content is relatively higher along the north-eastern side extending to the centre of the field including some area of the western corner of the field shown by dotted lines in figure 17a and dotted arrows in figure 17b. The deepsoil clay content somewhat follows a similar pattern. This spatial distribution of clay fairly reflected in the ECa maps as those areas showed higher ECa response where the clay content is higher shown by dotted lines and arrows in figure 15. In addition, the clay content in three depths found lower along the southern border extending to centre of the field which is fairly reflected by relatively lower ECa response in the ECa maps.

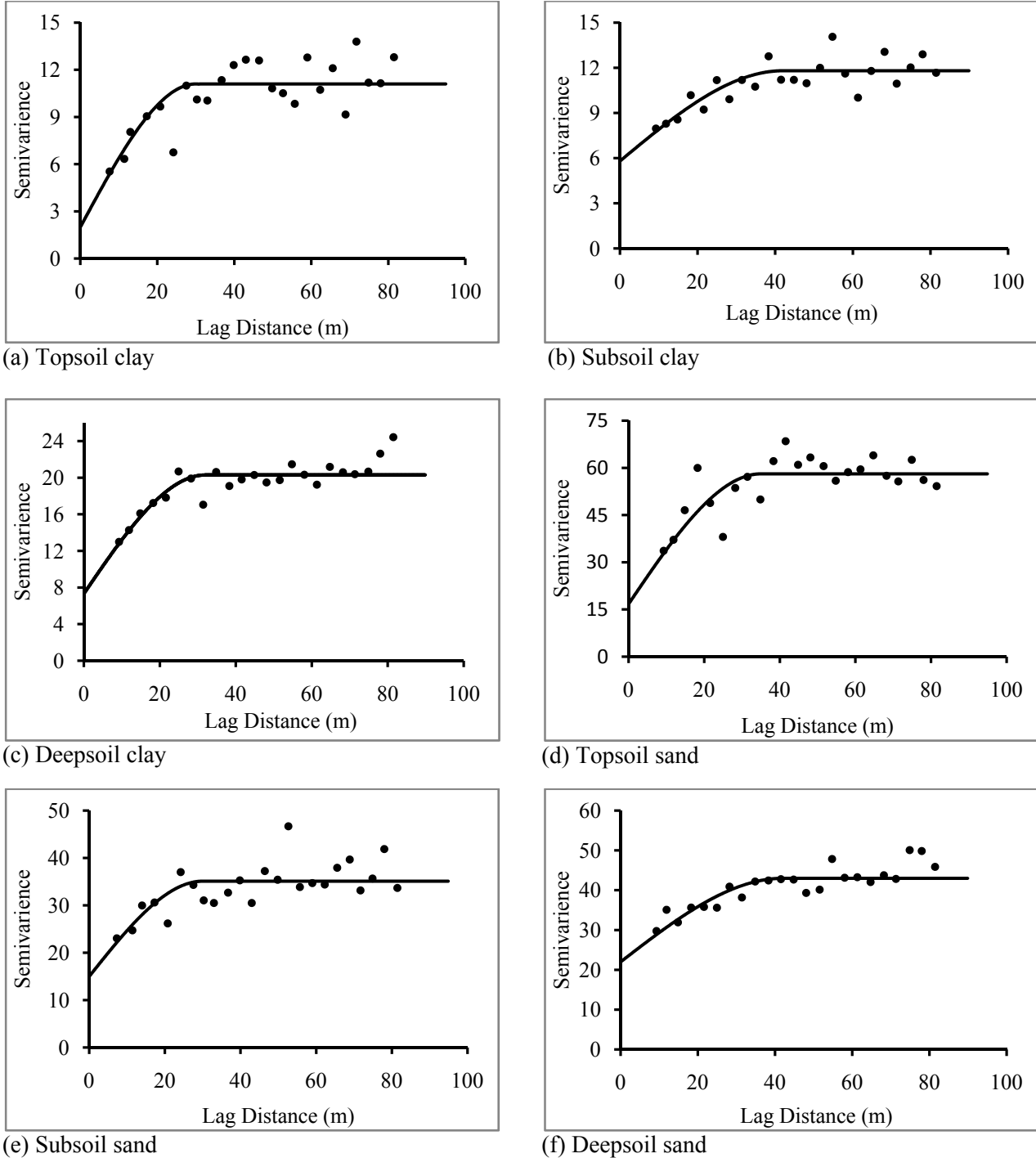


Figure 16. Variograms of clay (a, b and c) and sand fractions (d, e and f) in the terrace site

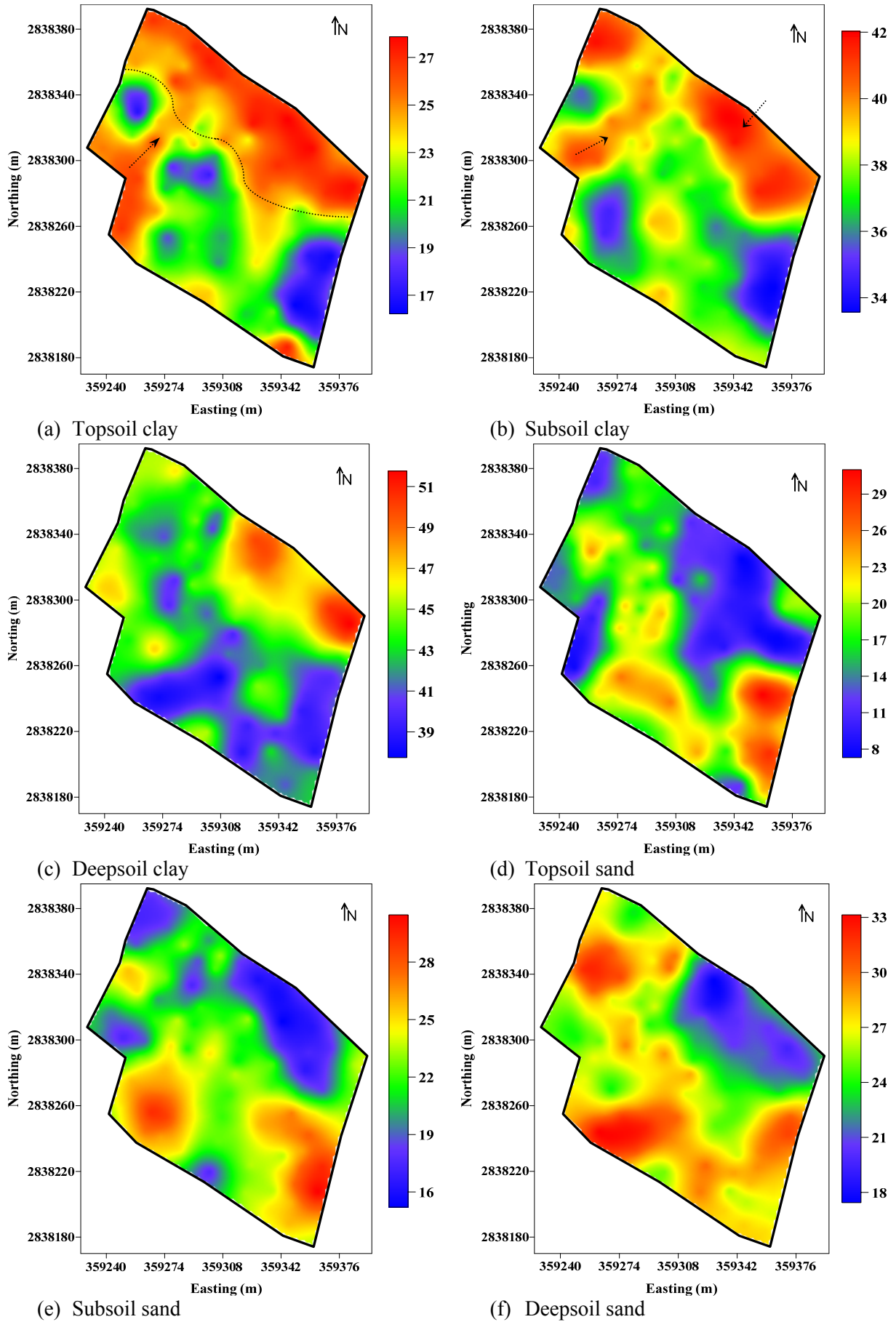


Figure 17. Kriged estimates of clay (a, b, c) and sand (d, e, f) content (%) in the terrace site

The possible causes of clay distribution in the topsoil might include: a) the south-western side of the field is biologically more active as this part of the field get organic matter, and drainage usually follow south-west to north-east which cause the finer material (silt and clay) to be moved in that direction by drainage and also during puddling of the field, and b) the unstable silty topsoil along the north-eastern side is eroded during the moonsoon as there flows a stream of narrow tributary which occasionally overflows due to heavy moonsoon rain or excess water from its river source.

#### 4.1.3.3 Mapping the chemical soil properties

The fitted spherical variogram of the chemical properties, i. e., pH, CEC,  $\text{Ca}^{2+}$  and  $\text{Mg}^{2+}$ , are shown in figure 18 while the model parameters are listed in table 8. The omni-directional range of autocorrelation is 32 m and 30 m for pH and CEC respectively. But the extent of autocorrelation for the exchangeable ions  $\text{Ca}^{2+}$  and  $\text{Mg}^{2+}$  is 25 m. The relative nugget effect is relatively high (pH – 60 %,  $\text{Ca}^{2+}$  - 46 % and  $\text{Mg}^{2+}$ - 57 % except the CEC (30 %)) which means that the inexplicable or short distance random variations are considerable. Moreover, the higher RNE's of pH,  $\text{Ca}^{2+}$  and  $\text{Mg}^{2+}$  indicates that their spatial variation are moderately structured by the fitted models. The maps of kriged predictions are shown in figure 19.

Table 8. Model parameters of omni-directional spherical variograms for the chemical properties

Variable	Variogram parameters			
	$C_0$ , nugget variance $(\text{mSm}^{-1})^2$	C, sill $(\text{mSm}^{-1})^2$	h, range (m)	RNE, relative nugget effect (%)
pH	0.12	0.02	32	60
CEC	1	3.3	30	30
$\text{Ca}^{++}$	0.18	0.39	25	46
$\text{Mg}^{++}$	0.04	0.07	25	57

The soil acidity varies regularly throughout the field; the distribution is somewhat polygonal in nature. The relative nugget effect is 60 % which means random variation of acidity over the site is considerable. The CEC content shows relatively less variation, its spatial distribution is approximately strongly structured, i.e. RNE 30 %. The kriged map revealed that CEC is higher in the west and north corners, and lower at the eastern size of the field shown by broken and solid arrows respectively in figure 19b. This higher CEC in those areas might be caused by relatively higher clay content and organic matter. Nevertheless, the mean CEC of the reference site is found to be  $12.63 \text{ cmol}^+ \text{ kg}^{-1}$ . The organic matter level for majority area of the field is quite low which means that CEC mostly caused by the clay. CEC is the total sum of

exchangeable cations that a soil can absorb or hold. The exchange capacity is mainly dependent on the type and amount of clay minerals, sesquioxides and organic matter. In highly weathered and acidic terrace soil, clay fractions are dominated by mica and kaolinite which cause the CEC to be relatively low than the adjoining floodplain (Moslahuddin et. al., 2008). The exchangeable  $\text{Ca}^{2+}$  showed somewhat similar distribution as the CEC (Figure 19c). The  $\text{Mg}^{2+}$  showed a nugget variance close to zero which means that hardly any changes take place within distance smaller than 25 m of an autocorrelation radius. The kriged map shows two major spatial distributions with a patch of lower  $\text{Mg}^{2+}$  in the eastern side shown by arrow in figure 19d. The exchangeable cations show a moderately structured spatial distribution as revealed from their respective relative nugget effect. Moreover, the spatial distribution for pH and  $\text{Ca}^{2+}$  showed approximate periodicity or recurrence at regular interval which is evident from their kriged maps shown in figure 19a and 19c respectively.

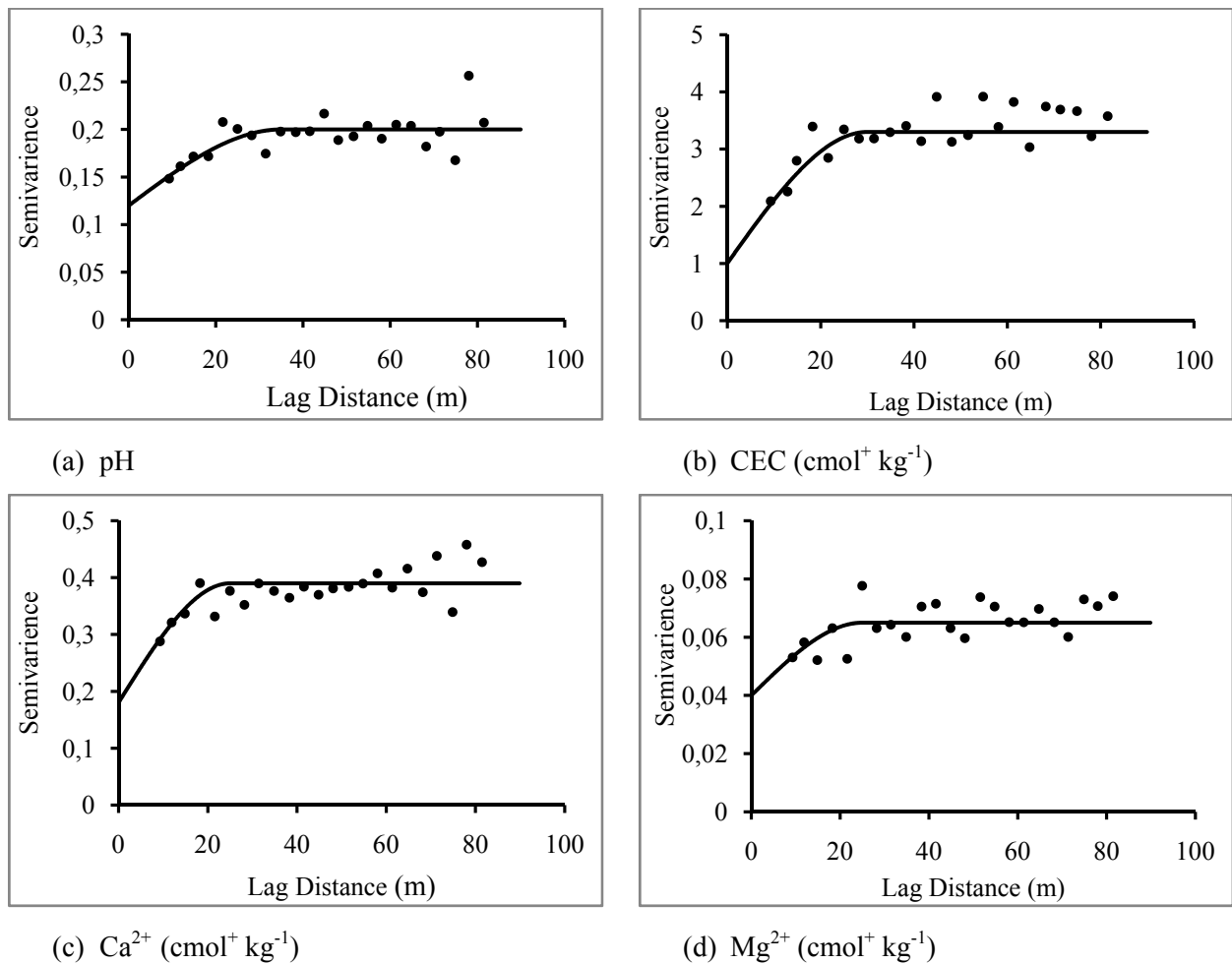
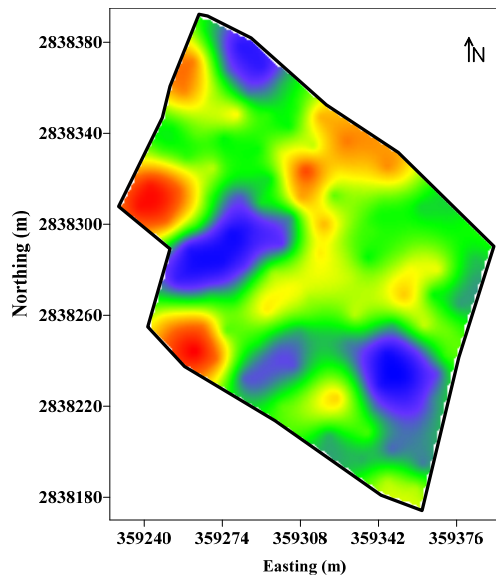
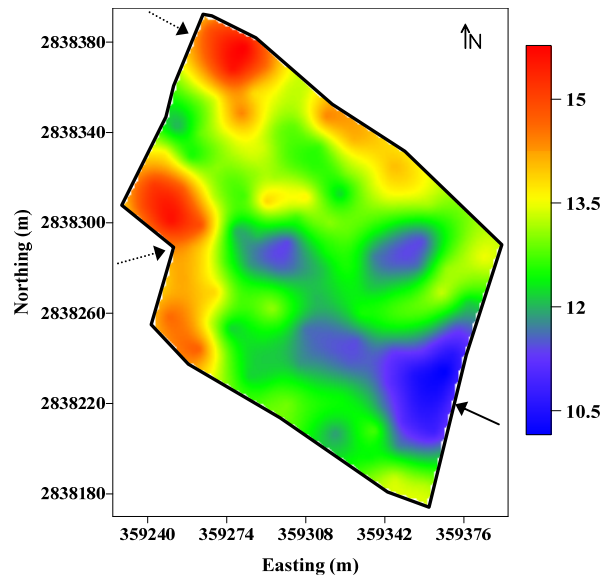


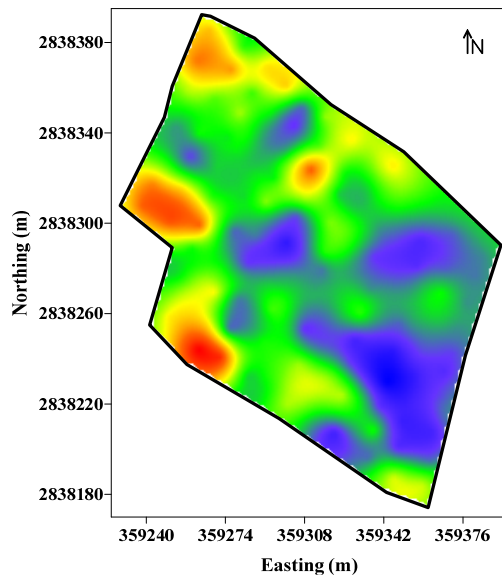
Figure 18. Variograms of a) pH, b) CEC, c)  $\text{Ca}^{2+}$  and d)  $\text{Mg}^{2+}$  in the terrace site



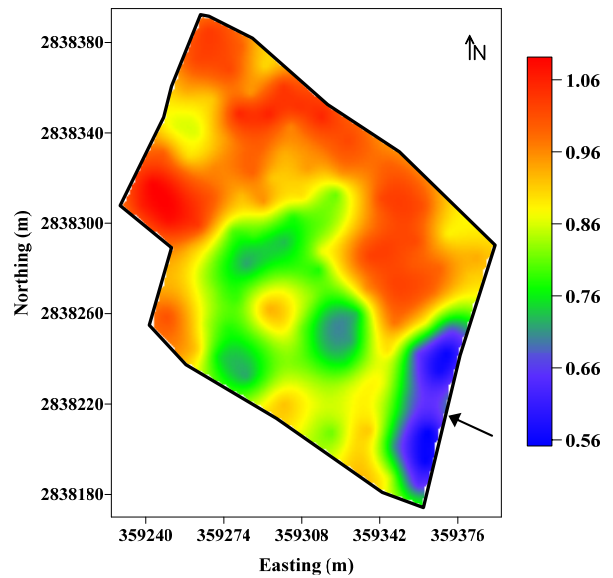
(a) pH



(b) CEC ( $\text{cmol}^+ \text{kg}^{-1}$ )



(c)  $\text{Ca}^{2+}$  ( $\text{cmol}^+ \text{kg}^{-1}$ )



(d)  $\text{Mg}^{2+}$  ( $\text{cmol}^+ \text{kg}^{-1}$ )

Figure 19. Kriged estimates of the topsoil chemical properties, a) pH, b) CEC, c)  $\text{Ca}^{2+}$  and d)  $\text{Mg}^{2+}$  in the terrace site

## 4.2 Floodplain site

### 4.2.1 Descriptive statistics

#### 4.2.1.1 Soil properties

The soil properties were approximately of symmetrical distribution. This was further confirmed by their respective coefficients of skewness (Table 9 and 10). The frequency distribution of the selected soil properties are shown in figure 20. The soil properties in the floodplain site showed a large spatial variation as explicated by their large variance and coefficients of variation.

Table 9. Descriptive statistics of textural fractions in floodplain site, n = 20

<b>Top soil (0-30 cm)</b>									
	Mean	Median	Min	Max	Variance	Std. dev.	Skewness	Kurtosis	CV (%)
Clay	21.4	20.6	9.4	38.2	47.29	6.88	0.74	0.79	32
Silt	70.6	74.9	43.7	80.4	88.88	9.43	-1.40	1.97	13
Sand	8.0	5.2	1.0	42.3	106.96	10.34	2.51	6.52	129
<b>Subsoil (30-60 cm)</b>									
Clay	13.9	13.5	7.40	21.70	19.74	4.44	0.19	-1.25	32
Silt	67.7	70.6	43.40	81.10	149.39	12.22	0.55	-1.23	18
Sand	18.4	12.60	1.20	44.40	206.08	14.36	-0.27	-0.10	78
<b>Deepsoil (60-90 cm)</b>									
Clay	12.7	12.3	4.9	34.4	40.02	6.33	2.10	6.82	50
Silt	69.7	77.6	31.7	83.8	237.85	15.42	-1.19	-0.46	22
Sand	17.6	12.9	1.0	63.4	273.83	16.55	1.34	1.65	94

The mean particle size distribution of the topsoil and subsoil corresponded mainly to silt loam texture class while for the deepsoil 80 % observations mainly possess silt loam texture class and the remaining belongs to silt texture class (Figure 21). The mean content of clay in the topsoil is 21.4 % while for subsoil 13.9 % and deepsoil 12.7 % (Table 9). Furthermore, the CV's of the particle distribution (13 - 129 %) for all the observations showed that there remains considerable variation in the content of particle distribution in three depth increments, mostly for the sand fractions in the floodplain site.

Table 10. Descriptive statistics of topsoil chemical properties in the floodplain site, n = 20

Variable	Units	Mean	Median	Min	Max	Variance	Std. dev.	Skewness	Kurtosis	CV (%)
pH water		6.64	6.67	6.35	6.85	0.02	0.14	-0.71	0.51	2
Org. C	g kg <sup>-1</sup>	30.62	30.48	20.31	40.66	36.0	6.0	-0.40	0.20	20
Total N	g kg <sup>-1</sup>	0.73	0.44	0.20	2.07	0.34	0.58	1.34	0.28	78
Na <sup>+</sup>	cmol <sup>+</sup> kg <sup>-1</sup>	0.67	0.64	0.47	0.94	0.01	0.58	0.75	1.87	15
CEC	cmol <sup>+</sup> kg <sup>-1</sup>	21.34	20.75	18.15	23.34	4.16	2.04	-0.50	-1.15	9
Ca <sup>2+</sup>	cmol <sup>+</sup> kg <sup>-1</sup>	12.76	12.47	7.22	17.31	4.35	2.09	-0.26	2.26	16
K <sup>+</sup>	cmol <sup>+</sup> kg <sup>-1</sup>	0.10	0.11	0.07	0.14	0.00	0.02	-0.11	-0.02	15
ECe	dS m <sup>-1</sup>	0.03	0.03	0.02	0.05	0.00	0.01	0.06	-0.94	23

The examined chemical properties showed a large within field variability for all the properties except pH which was further explained by their relatively higher CV's (Table 10). Soils in the floodplain site featured slightly acidic (mean pH 6.64) and medium level of organic C (mean 30.62 g kg<sup>-1</sup>) which varied from 20.31 to 40.66 g kg<sup>-1</sup> and high level of CEC (mean 21.34 cmol<sup>+</sup> kg<sup>-1</sup>) was found. The total N was found to be very low and the soluble salts were negligible. The level of exchangeable cation, Ca<sup>2+</sup> found high while the level of Mg<sup>2+</sup> and Na<sup>+</sup> were low.

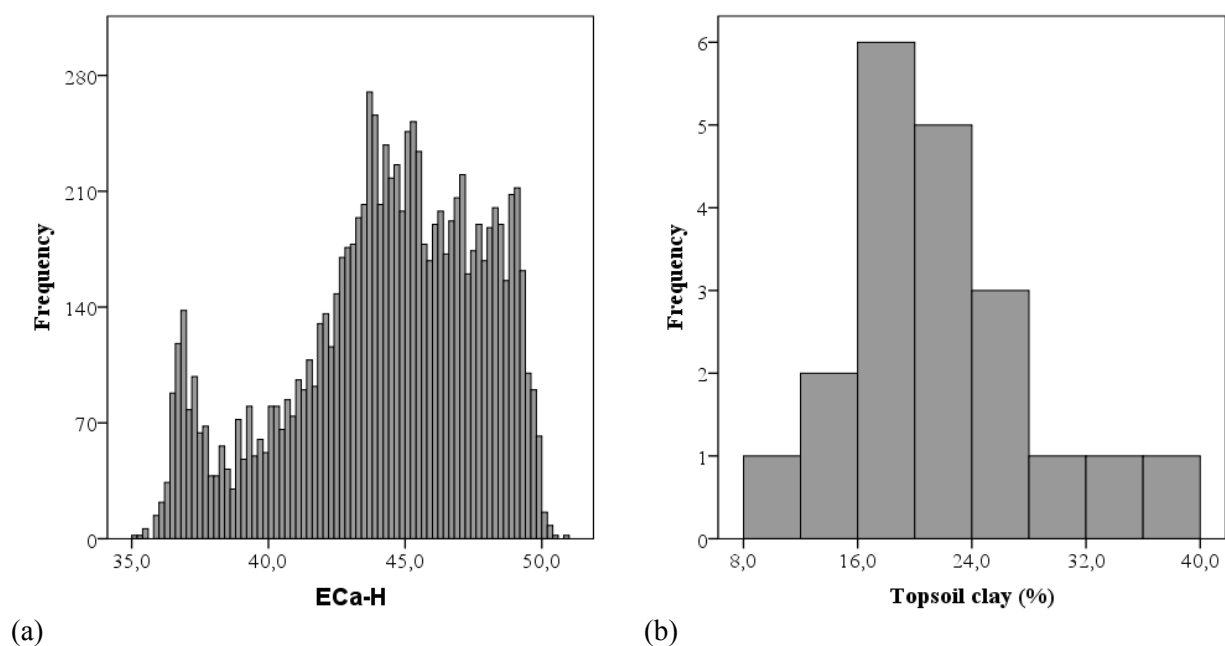
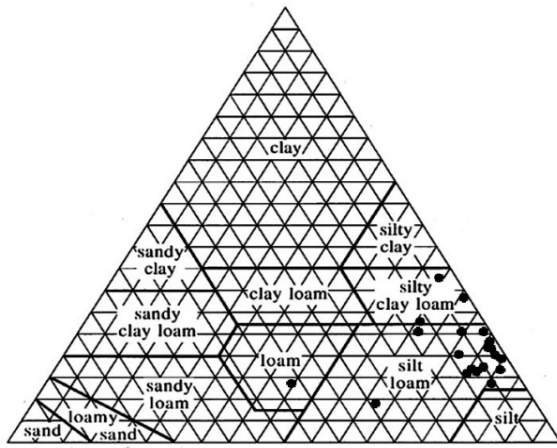
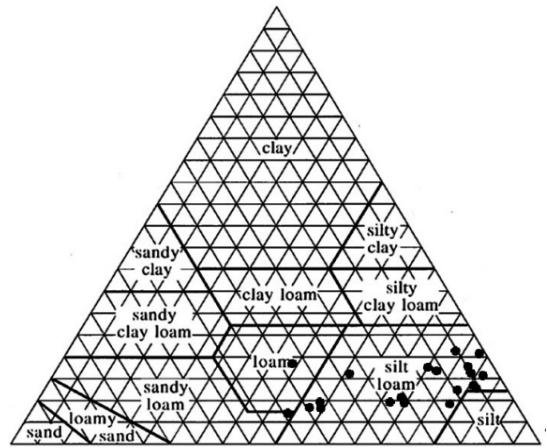


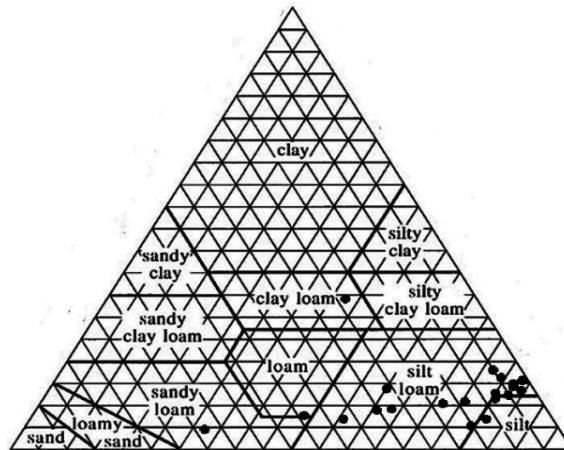
Figure 20. Histograms of a) ECa-H (mS m<sup>-1</sup>) and b) topsoil clay in the floodplain site



(a) Topsoil texture



(b) Subsoil texture



(c) Deepsoil texture

Figure 21. The distribution of textural class a) topsoil, b) subsoil and c) despoil in the USDA texture triangle in the floodplain site, n = 20

#### 4.2.2 Apparent electrical conductivity (ECa)

The ECa measurements were approximately of symmetrical distribution and skewed to the left. The ECa readings were ranged from 35.1 to 50.8 and 33.8 to 47.4 mS m<sup>-1</sup> for the horizontal and vertical orientation respectively in the floodplain site (Table 11). The readings of ECa-H were slightly larger than those of the simultaneous ECa-V. The coefficients of variations were in the same order in both orientations. The two orientations ECa responses were well correlated with a positive linear correlation coefficient of  $r = 0.90$ .

Table 11. Descriptive statistics of ECa (mS m<sup>-1</sup>) measurements in floodplain site

Variable	n	Mean	Median	Min	Max	Variance	Std. dev.	Skewness	Kurtosis	CV (%)
ECa-H	9,670	44.3	44.7	35.1	50.8	12.25	3.50	0.56	-0.42	8
ECa-V	10,515	41.8	42.3	33.8	47.4	11.27	3.35	-0.65	-0.33	8

ECa-H and ECa-V (mS m<sup>-1</sup>), apparent ECa measured in the horizontal and vertical mode respectively

#### 4.2.3 Correlation coefficients of ECa with textural and soil chemical properties

Pearson product moment ( $r$ ) correlations were performed between ECa and textural fractions, and topsoil chemical properties and ECa of the floodplain site (Table 12 and 13). The scatter plots between ECa and topsoil clay are shown in figure 22. The best positive correlation coefficient ( $r = 0.66$ ) occurred for ECa-H and topsoil clay, and the correlation for ECa-V ( $r = 0.61$ ) nearly coincided. The correlations for subsoil and deepsoil were found to be lower for the horizontal orientation. For the vertical orientation, the deepsoil clay responded moderately with a correlation coefficient of  $r = 0.45$  which is  $r = 0.33$  for subsoil clay. The correlations between ECa and textural fractions were found relatively lower except the topsoil which might be caused due to decreased amounts of clay in the sub- and deepsoil. In addition, since ECa is a function of number of soil properties the low weight of  $r$  values in the floodplain site (non-saline) indicated that factors other than texture, such as soil moisture or CEC might had effect for the conductivity variations (Sudduth et. al., 2001). However, the association between ECa and the examined chemical properties were reflected by their correlation coefficient as shown in table 13. Weak correlation coefficients were found for all the chemical properties except the organic C ( $r = 0.60$  and  $r = 0.48$  for the ECa-H and ECa-V respectively). The topsoil organic C correlated good with ECa due to relatively higher level of organic matter in the floodplain site.

Table 12. Pearson correlations (r) of ECa and textural fractions in the floodplain site, n = 20

Variable	ECa-H	ECa-V	T_clay	S_clay	D_clay	T_sand	S_sand	D_sand	T_silt	S_silt	D_silt
ECa-H	1	0.90**	0.66**	0.23	0.26	-0.42*	0.03	0.16	-0.08	-0.12	-0.28
ECa-V		1	0.61**	0.33	0.45*	-0.36	-0.12	-0.04	0.01	0.02	-0.14
T_clay			1	0.36	0.15	-0.46*	-0.08	-0.12	-0.23	-0.04	0.07
S_clay				1	0.38	-0.25	-0.60**	-0.41	0.01	0.34	0.28
D_clay					1	-0.40	-0.49*	-0.36	0.33	0.44	-0.02
T_sand						1	0.14	0.57**	-0.76**	-0.08	-0.45*
S_sand							1	0.41	-0.10	-0.96**	-0.24
D_sand								1	-0.54*	-0.33	-0.92**
T_silt									1	0.11	0.44
S_silt										1	0.18
D_silt											1

ECa-H and ECa-V ( $\text{mS m}^{-1}$ ), apparent ECa measured in the horizontal and vertical mode respectively and  $P \leq 0.01^{**}$ ,  $0.05^{*}$ .

Table 13. Pearson correlations (r) of ECa and topsoil chemical properties, n = 20

Variable	ECa-H	ECa-V	pH	O C	Total N	ECe	Na <sup>+</sup>	CEC	K <sup>+</sup>	Ca <sup>2+</sup>
ECa-H	1	0.90**	0.02	0.60**	0.39	-0.11	0.03	-0.34	-0.16	-0.02
ECa-V		1	0.16	0.48*	0.49*	0.09	-0.07	-0.32	-0.09	0.04
pH			1	-0.28	0.21	0.63**	-0.29	-0.07	-0.22	0.20
OC				1	0.21	-0.04	0.21	-0.32	-0.01	0.15
Total N					1	0.10	-0.02	0.06	0.13	-0.03
ECe						1	-0.20	0.06	-0.25	0.37
Na <sup>+</sup>							1	0.17	-0.11	0.56**
CEC								1	-0.03	0.11
K <sup>+</sup>									1	-0.14
Ca <sup>2+</sup>										1

ECa-H and ECa-V ( $\text{mS m}^{-1}$ ), apparent ECa measured in horizontal and vertical mode respectively; pH water, 1 : 2.5; OC, % organic carbon; Total N ( $\text{g kg}^{-1}$ ); CEC ( $\text{cmol}^{+} \text{kg}^{-1}$ ), cation exchange capacity; Exchangeable Ca<sup>2+</sup>, Na<sup>+</sup> and K<sup>+</sup> ( $\text{cmol}^{+} \text{kg}^{-1}$ ); ECe ( $\text{dS m}^{-1}$ ) and  $P \leq 0.01^{**}$ ,  $0.05^{*}$ .

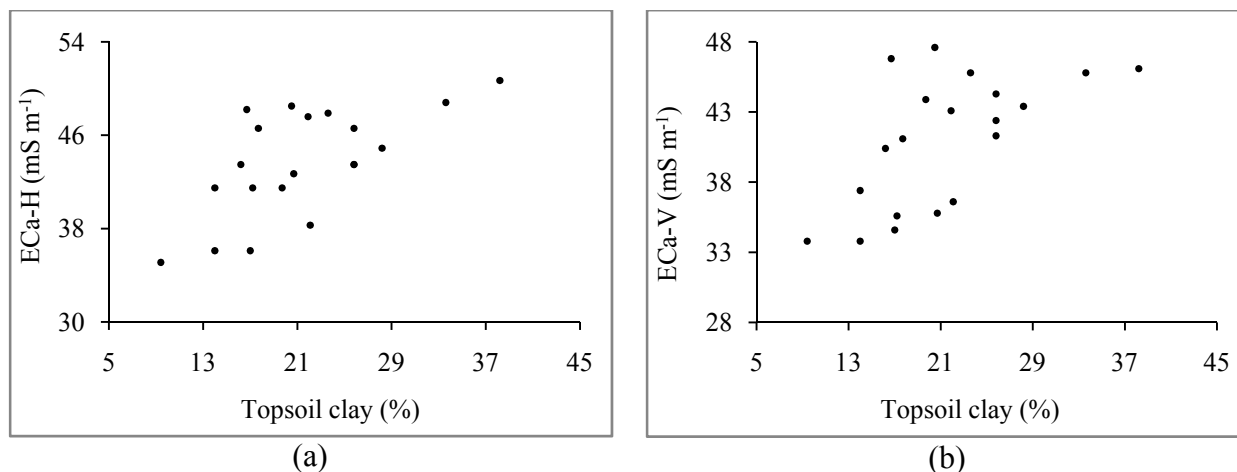


Figure 22. Scatter plots, a) of ECa-H and topsoil clay and b) ECa-V and topsoil clay in the floodplain site

#### 4.2.4 Mapping of ECa measurements

The ECa data sets were modeled with omni-directional double spherical variograms (Figure 23). The fitted models consisted 17.7 m and 16 m of separation distance at which spatial autocorrelation between data point pairs ceases for ECa-H and ECa-V respectively (Table 14). The relative nugget effect (RNE) was zero. The absence of nugget variance suggested that a strong spatial variability had been identified and hardly any variability was left at the characteristic distances smaller than the respective range. Ordinary kriging was used for the estimation and construction of the continuous surface ECa maps. The map of ECa-H and ECa-V was obtained with grid geometry of 1 by 1 m and showed similar pattern (Figure 24).

Table 14. Model parameters of omni directional double spherical variograms for ECa

Variogram parameters						
Variable	C <sub>0</sub> , nugget variance (mSm <sup>-1</sup> ) <sup>2</sup>	C <sub>1</sub> , sill (mSm <sup>-1</sup> ) <sup>2</sup>	C <sub>2</sub> , sill (mSm <sup>-1</sup> ) <sup>2</sup>	h <sub>1</sub> , range (m)	h <sub>2</sub> , range (m)	RNE, relative nugget effect (%)
ECa-H	0.0	0.72	0.13	17.7	4.0	0.0
ECa-V	0.0	0.73	0.10	16	3.0	0.0

The soil ECa maps were prepared for ECa-H with topsoil clay and sand content superimposed on it, and ECa-V with deepsoil clay superimposed on it. The survey provided representative ECa map of the spatial extent and magnitude of clay and sand content of top- and deepsoil. Furthermore, the EM38 data collected in the horizontal dipole mode were slightly more

predictive than the vertical dipole mode data for topsoil but for deepsoil the vertical orientation was better suited. The level of clay is relatively higher in the northern side of the field where the response of ECa is also found higher shown in figure 24a. In addition, it also illustrates that the finer materials tend to move north to south of the field shown by dotted lines with arrows in the map of ECa-H (Figure 24a) which might be caused due to direction of drainage which follow the same pathway. In the middle of the field, there are also zones of lower clay where the ECa was measured relatively lower shown by a dotted arrow in figure 24a.

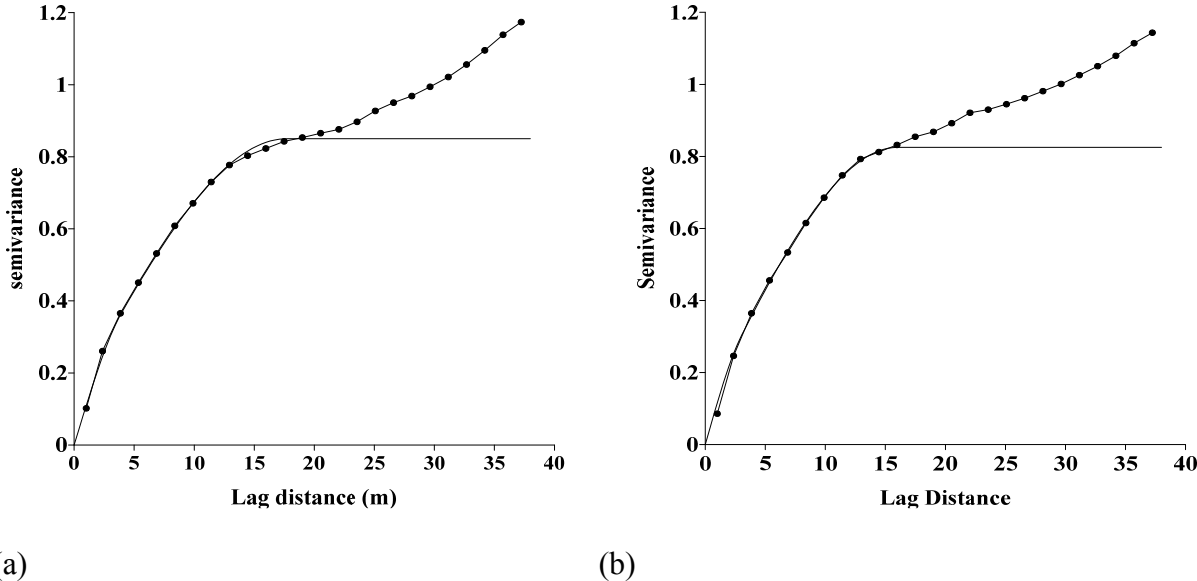
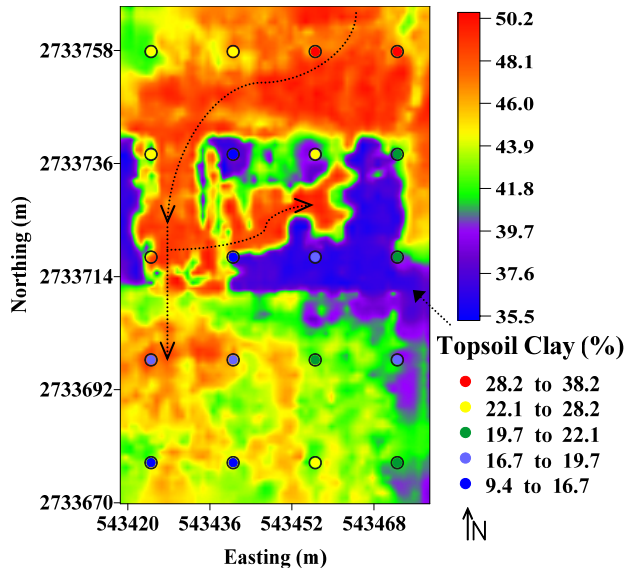
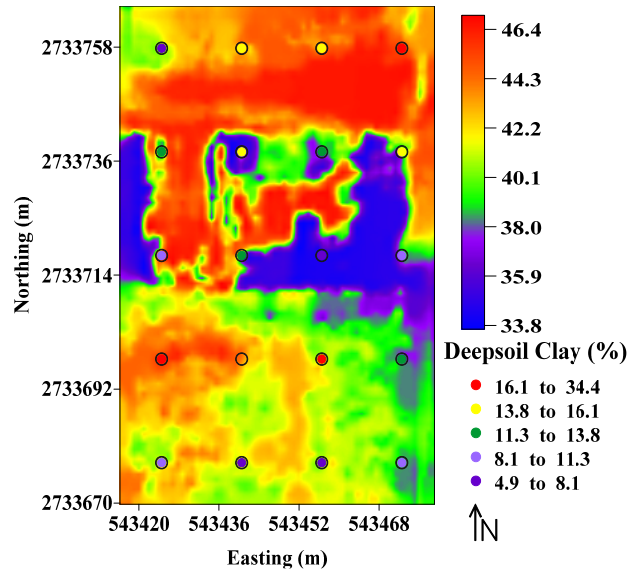


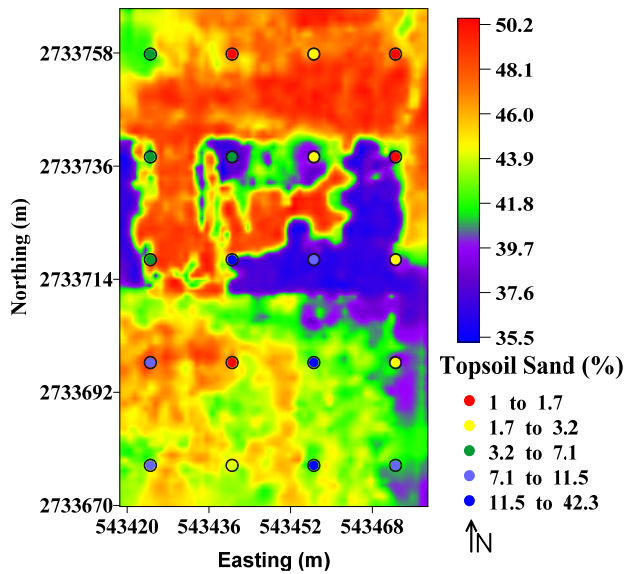
Figure 23. Variograms of the ECa-H and ECa-V in the floodplain site



(a) ECa-H



(b) ECa-V



(c) ECa-H

Figure 24. Interpolated values in  $\text{mS m}^{-1}$  for the ECa-H with a) topsoil clay and c) sand, and the ECa-V with b) deepsoil clay contents superimposed on the maps in the floodplain site

## 5. Comparison of EM38 conductivity response with soil properties in the terrace and floodplain site

The soil apparent electrical conductivity (ECa) readings from the non-invasive electromagnetic induction soil sensor, EM38, correlated best with texture from three depth increments (0-30 cm, 30-60 cm and 60-90 cm) and with four topsoil chemical properties (pH, CEC, Ca<sup>2+</sup> and Mg<sup>2+</sup>) in the terrace study site. For the floodplain site, the ECa readings correlated best with top- and deepsoil texture, and topsoil organic C. At the terrace site, the EM38 readings in the vertical orientation (ECa-V) point measurements ranged from 40 to 64 mS m<sup>-1</sup> while readings in the horizontal orientation (ECa-H) ranged from 32 to 53 mS m<sup>-1</sup> (Table 3). In the case of floodplain site, ECa-V continuous measurements ranged from 33.8 to 47.4 mS m<sup>-1</sup> and ECa-H measurements from 35.1 to 50.8 mS m<sup>-1</sup> (Table 11). In the terrace site, the EM38 response to soil conductivity was relatively higher for the vertical orientation than the horizontal orientation but in the floodplain site, the conductivity responded in the opposite way. The correlation coefficients between ECa-V and subsoil clay and sand were the highest ( $r = 0.78$  and  $r = -0.84$  respectively) for the terrace site. But in the floodplain site, the correlation coefficient between ECa-H and topsoil clay was the highest ( $r = 0.66$ ). These differences in the correlations among the two study sites could be related to their soil properties which differed fundamentally because of different parent material and soil forming process. The terrace site characterized by a considerable increase of clay content with depth having a Tertiary clayey substratum which is assumed to be of fluvial origin whereas the floodplain site was developed through alluvium deposits and sediments having a sandy substratum. The ECa-V map of the terrace site (Figure 15) fairly represents the spatial distribution of subsoil clay showing higher ECa response in the areas where level of clay is also higher. For the floodplain site, the surface ECa map (Figure 24) also showed a reasonable mutual integrity in terms of ECa response against respective textural fractions. The topsoil clay content overlaid in the ECa-H map clearly shows the positive spatial relation of ECa and clay. Among the chemical properties of the terrace site, four soil properties namely, pH, CEC and exchangeable Ca<sup>2+</sup> and Mg<sup>2+</sup> showed positive and significant correlation coefficients ( $r = 0.46$ ,  $r = 0.53$ ,  $r = 0.51$ , and  $r = 0.66$  respectively) with ECa-V. Other tested chemical properties, i.e., organic C, total N, available P, base saturation and K<sup>+</sup> did not show explicable correlations with the ECa measurements. For the floodplain site, most of the chemical properties did not show explicable correlation except topsoil organic C ( $r = 0.60$ ) which indicated that topsoil texture (clay) was main influencing soil property for the ECa readings. Nevertheless, these findings suggest that there is a potential of field scale ECa survey to map the spatial extent and magnitude of soil texture including key chemical properties (pH, CEC, Ca<sup>2+</sup> and Mg<sup>2+</sup>) through the EM38 sensor in the terrace soils, and soil texture and organic C in the floodplain soils of Bangladesh.

## 6. Conclusion

Electromagnetic induction (EMI) survey was conducted in the terrace and floodplain soils of Bangladesh by using a soil sensor, EM38. The soil apparent electrical conductivity (ECa) readings in the vertical orientation (ECa-V) of measurement ranged from 40 to 64 mS m<sup>-1</sup> while readings in the horizontal orientation (ECa-H) ranged from 32 to 53 mS m<sup>-1</sup> in the terrace site. In the floodplain site, the ECa-V readings ranged from 33.8 to 47.4 mS m<sup>-1</sup> and ECa-H readings from 35.1 to 50.8 mS m<sup>-1</sup>. The EM38 response to soil conductivity was relatively higher for the vertical orientation than the horizontal orientation in the terrace site. But in the floodplain site, the ECa-H response was slightly higher than the ECa-V. In the terrace site, the ECa readings correlated best with soil property such as top-, sub-, and deepsoil texture (clay and sand), and topsoil chemical property, i. e. pH, CEC, Ca<sup>2+</sup> and Mg<sup>2+</sup>. In the floodplain site, the ECa readings correlated best with top- and deepsoil texture, and topsoil organic C. A modest correlation was found in the terrace site between ECa-V and the subsoil clay ( $r = 0.78$ ), and ECa-V and the subsoil sand ( $r = - 0.84$ ). This might be caused due to the high amount of clay in the subsoil (about 40 %) and for the shallow Tertiary clay substratum. But in the floodplain site, the correlation between ECa-H and topsoil clay was the highest ( $r = 0.66$ ). This might be caused due to the clay content in the topsoil (>22 %) and the shallow sandy substratum. The variogram analysis revealed that a large portion of the total variation of soil property (about 70 %) was accounted for the spatially structured component of the variogram.

The study findings have brought an expectation that soil mapping through ECa measurement is possible in Bangladesh. For mapping, the ECa-V measurement in the terrace soil is more predictive than ECa-H while the ECa-H measurement in the floodplain soil is more predictive than ECa-V. The maps of ECa can fairly represent the spatial variation of soil properties. Thus provide useful information on soil texture, chemical fertility and organic matter content. The ECa map also provides a means of monitoring the spatial variation of soil properties that potentially influence the crop production. The ECa maps can also guide directed soil sampling with the purpose of updating the existing soil maps of Bangladesh.

## 7. Recommendations

1. The field-scale application of EMI survey could be a quick and less expensive tool for finding soil spatial variation (texture and plant nutrients map) in Bangladesh. The EMI based survey in combination with the prevailing updating scheme of national soil maps could be useful in the context of ECa directed soil sampling, time and money to accelerate the retarded updating activities of the existing semi-detail polygon maps.
2. Delineation of site-specific management zones through conducting similar research in relatively heterogeneous soils in combination with yield data might help the interpretation of the relationship between the EM38 derived maps and yield variations that may lead to the adoption of site-specific management practices.
3. Soil moisture content is one of the key limitations against the agricultural practices in the terrace areas. The spatial and temporal variability of moisture content could be identified at different depth using EM38 which might substantially estimate the massive irrigation requirement during drier periods of crop (rice and winter crops) cultivation.
4. Clay content, soil moisture content, CEC, clay mineralogy, soil pore size and distribution, and soil salinity are some of the factors that affect ECa. Therefore, to examine the effect of all these properties both in dry and moist condition with repetitive seasonal study should be performed to understand comprehensively the application potential and extent of use of EM38 in Bangladesh.
5. The study was premeditated and deliberately confined to small area for the terrace site and even rather small for the floodplain site. The results from both study sites showed potential for further exploration and extension of the relevant study. A more deliberately weighted and adapted frameworks could be implemented over large areas of different soil type and conditions. This will guide to generalize the findings and for definitive suggestions to impart for Bangladesh.
6. The lateral spatial extent and depth of clayey substratum of the characteristic Madhupur clay beneath the subsoil of terrace areas of Bangladesh could be mapped by EM38. The floodplain soils characterized by a ploughpan due to extensive mono-culture of rice, the depth variability and compactness of this hardpan could be identified by EMI based survey.
7. Bangladesh has about 2.8 million ha of land affected by salinity and poor quality water. The EMI survey for saline soils has already been a proven tool and there exist a great potential to characterize the saline soils through EM38.

## 8. Reference

- Adamchuk, V. I., Hummel, J. W., Morgan, M. T., Upadhyaya, S. K. 2004. On-the-go soil sensors for precision agriculture. *Computers and Electronics in Agriculture* 44: 71-91.
- Ali, M. Y., Rahman, M. A., Quayyum, M. A. and Islam, M. B. 2007. Improved adaptive capacity to climate change for sustainable livelihoods in the agricultural sectors - The case of High Barind Tract: BARI-FAO collaborative program. On-Farm Research Division (OFRD), Bangladesh Agricultural Research Institute (BARI), Gazipur, Bangladesh.
- Auerswald, K., Simon, S. and Stanjek, H. 2001. Influence of soil properties on electrical conductivity under humid water regimes. *Soil Science* 166: 382-390.
- BARC, 2005. Bangladesh Agricultural Research Council, Ministry of Agriculture, Bangladesh.
- BBS, 2008. Statistical Pocketbook of Bangladesh, 2008. Bangladesh Bureau of Statistics, Government of the People's Republic of Bangladesh, Dhaka, Bangladesh.
- Benson, A. K., Payne, K. L. and Stubben, M. A. 1997. Mapping groundwater contamination using DC resistivity and VLF geophysical methods - A case study. *Geophysica* 62 (1): 80-86.
- Billal, H. M. 2008. EM38 for measuring and mapping soil moisture in a cracking clay soil. PhD thesis. Department of Geography and planning, University of New England, Australia.
- Biswas, T. D. and Mukherjee, S. K. 1987. Text Book of Soil Science, p. 291. Tata Mc Grew-Hill Publishing Co. Ltd. New Delhi, India.
- BMDA, 2010. Barind Multipurpose Development Authority, Ministry of Agriculture, Bangladesh. <http://bmda.gov.bd/> (Read June 15, 2010).
- Brammer, H. 1996. The Geography of the soils of Bangladesh. The University Press Limited, Dhaka, Bangladesh.
- Brammer, H. 2002. Land use and land use planning in Bangladesh. The University Press Limited, Dhaka, Bangladesh.
- Bray, R. H. and Kurtz, L. T. 1945. Determination of total, organic, and available forms of phosphorus in soils. *Soil Science* 59: 39-45.
- Brevik, E. C., Thomas, E. F. and Lazari, A. 2006. Soil electrical conductivity as a function of soil water content and implications for soil mapping. *Precision Agriculture* 7: 393-404.
- Bronson, K. F., Booker, J. D., Officer, S. J., Lascano, R. J., Maas, S. J., Searcy, S. W. and Booker, J. 2005. Apparent electrical conductivity, soil properties and spatial covariance in the U.S. Southern High Plains. *Precision Agriculture* 6: 297-311.
- Burrough, P. A. and McDonnell, R. A. 1998. Principals of geographical information systems. Oxford University Press, Oxford.

- Burrough, P.A. 1993. Soil variability: a late 20<sup>th</sup> century view. *Soil and Fertilizers* 56: 529-562.
- Cambardella, C. A., Moorman, T. B., Novak, J. M., Parkin, T. B., Karlen, D. L., Turco, R. F. and Konopka, A. K. 1994. Field-scale variability of soil properties in central Iowa soils. *Soil Science Society of America Journal* 58: 1501-1511.
- Chapman, H. D. 1965. Cation-exchange capacity. In: C. A. Black, editor, *Methods of soil analysis - Chemical and microbiological properties*. *Agronomy* 9: 891-901.
- Cockx, L. 2010. High resolution soil inventory using a dual signal electromagnetic induction sensor. PhD thesis, Department of soil management, Ghent University.
- Corwin D. L. and Lesch, S. M. 2005. Apparent soil electrical conductivity measurements in agriculture. *Computers and Electronics in Agriculture* 46: 181-202.
- Corwin, D. L. and Lesch, S. M. 2003. Application of soil electrical conductivity to precision agriculture: theory, principles and guidelines. *Agronomy Journal* 95: 455-471.
- Corwin, D. L., Lesch, S. M. Osterb, J. D. and Kaffka, S. R. 2006. Monitoring management induced spatio-temporal changes in soil quality sampling directed by apparent electrical conductivity. *Geoderma* 131: 369-387.
- Day, P. R. 1965. Particle fractionation and particle-size analysis. *Methods of soil analysis*, p. 545-567, C. A. Black, Ed. *Agronomy No. 1*. American Society of Agronomy, Madison, WI.
- Erickson, B. 2004. Field experience validates on-the-go soil pH sensor. Site-specific management center, Purdue University. (Read June 15, 2010)  
[http://www.agriculture.purdue.edu/ssmc/frames/ssmc%20newsletter12\\_04.pdf](http://www.agriculture.purdue.edu/ssmc/frames/ssmc%20newsletter12_04.pdf)
- FAO-UNESCO, 1988. FAO-UNESCO soil map of the world. Revised legend, FAO, Rome.
- Fertilizer Recommendation Guide, 2005. Bangladesh Agricultural Research Council, Ministry of Agriculture, Bangladesh.
- Friedman, S.P. 2005. Soil properties influencing apparent electrical conductivity: a review. *Computers and electronics in Agriculture* 46: 45-70.
- Freeland, R.S., Yoder, R.E., Ammons, J.T. and Leonard, L.L. 2002. Mobilized surveying of soil conductivity using electromagnetic induction. *Applied Engineering in Agriculture* 18: 121-126.
- Gee, G. W., and J. W. Bauder, 1986. Particle size analysis, p. 383-411, In: A. Clute, editor, *Methods of soil analysis, part 1. Physical and mineralogical methods*. *Agronomy monograph* 9. American Society of Agronomy, Madison, WI.
- Goovaerts, P. 1997. *Geostatistics for natural resources evaluation*. Oxford University Press, New York.

- Hendershot, W. H. and Duquette, M. 1986. A simple barium chloride method for determining cation exchange capacity and exchangeable cations. *Soil Science Society America Journal* 50: 605-608.
- Hendrickx, J. M. H. and Kachanoski, R. G. 2002. Solute content and concentration-indirect measurement of solute concentration-nonintrusive electromagnetic induction. In: Dane, J.H., Topp, G.C., editors, *Methods of Soil Analysis, Part 4*, p. 1297-1306 - Physical Methods. Book Ser. 5. Soil Science Society of America, Madison, WI, USA.
- Ibrahim and Baset, 1973. Reconnaissance soil survey of sadar sub-division, Dinajpur district. Soil Resource Development Institute (SRDI), Ministry of Agriculture, Bangladesh.
- Islam, M. M. 2009. ORBit Research Group - Soil Spatial Inventory Techniques, Department of Soil Management, Ghent University, Belgium.
- Knudsen, D., Peterson, G. A. and Pratt, P. F. 1982. Lithium, sodium and potassium. In: A. L. Page et. al., editors. *Methods of soil analysis*, Pages 247-262. Part 2. Agronomy No. 9. American Society of Agronomy, Madison, WI.
- Kühn, J., Brenning, A., Wehrhan, M., Koszinski, S. and Sommer, M. 2009. Interpretation of electrical conductivity patterns by soil properties and geological maps for precision agriculture. *Precision Agriculture* 10: 490-507.
- Lesch, S.M., Corwin, D. L. and Robinson, D. A. 2005. Apparent soil electrical conductivity mapping as an agricultural management tool in arid zone soils. *Computers and Electronics in Agriculture* 46: 351–378.
- Lin, H. S., Wheeler, D., Bell, J. and Wilding, L. 2005. Assessment of soil spatial variability at multiple scales. *Ecological Modelling* 92 (1): 271-290.
- McBratney, A. B., Whelan, B. M., Ancev, T., and Bouma, J. 2005. Future directions of precision agriculture. *Precision Agriculture* 6: 7-23.
- McBride, R. A., Gordon, A. M. and Shrive, S. C. 1990. Estimating forest soil quality from terrain measurements of apparent electrical conductivity. *Soil Science Society of America Journal* 54: 290-293.
- McNeill, J. D. 1980. Electromagnetic terrain conductivity measurement at low induction numbers. In: Geonics Limited Library ([www.geonics.com](http://www.geonics.com)), editor, Technical note, TN-6. Mississauga, Canada.
- Moral, F. J., Terron, J. M. and Marques, J. R. 2010. Delineation of management zones using mobile measurements of soil apparent electrical conductivity and multivariate geostatistical techniques. *Soil & Tillage Research* 106: 335–343.
- Moslehuddin, A. Z. M., Habibullah, Moniruzzaman, M. and Egashira, K. 2008. Mineralogy of Soils from Different Agroecological Regions of Bangladesh: Region 25 - Level Barind Tract and Region 27-North-eastern Barind Tract. *Journal of Faculty of Agriculture, Kyushu University*, 53 (1): 163–169.

- Nelson, D. W. and Sommers, L. E. 1996. Total carbon, organic carbon, and organic matter. In: A. L. Page, editor, *Methods of soil analysis*, p. 961-1010, part 2. Chemical and microbiological properties. American Society of Agronomy, Madison, WI.
- Oliver, M. A. 1987. Geostatistics and its application to soil science. *Soil Use and Management* 3: 8-20.
- ORBit, 2010. The use of electromagnetic induction in soil management applications. Research Group Soil Spatial Inventory Techniques, Department of Soil Management, Ghent University. <http://www.soilman.ugent.be/orbit>, (Read June 15, 2010).
- Orr, A., Riches, Mortimer, C. R., Harris, A. M. and Mazid, M. A. 2008. Farm-level opportunities for increasing productivity and income in the High Barind Tract: a synthesis. In: Riches, C. R., Harris, D. and Hardy, B., editors, *Improving agricultural productivity in Rice-Based systems of the high Barind Tract of Bangladesh*, p. 9-25. International Rice Research Institute (IRRI), Philippines.
- Pannatier Y. 1996. *VARIOWIN: Software for Spatial Data Analysis in 2D*. Springer-Verlag, New York.
- Raphael, A.V.R. 2002. Development of a proximal soil sensing system for the continuous management of acid soil. PhD thesis, Department of Agricultural Chemistry and Soil Science, The University of Sydney, Australia.
- Rashid, H. Er., 1991. *Geography of Bangladesh*, University Press Limited, Dhaka.
- Rhoades, J. D., Chanduvi, F. and Lesch, S. 1999. Soil salinity assessment: methods and interpretation of electrical conductivity measurements. *FAO: Irrigation and Drainage Paper-57*, p. 1-150. Food and Agriculture Organization of the United Nations, Rome, Italy.
- Rhoades, J. D., Manteghi, N. A., Shouse, P. J. and Alves, W. J. 1989. Soil electrical conductivity and soil salinity: New formulations and calibrations. *Soil Science Society America Journal* 53: 433-439.
- Robinson, D. A., Lebron, I., Lesch, S. M. and Shouse, P. 2004. Minimizing drift in electrical conductivity measurements in high temperature environments using the EM-38. *Soil Science Society America Journal* 68: 339-345.
- Saheed, S.M. 1992. Soil Survey: perspective and strategies for the 21<sup>st</sup> century. In: J. A. Zinck, editor, *An International Workshop for Heads of National Soil Survey Organizations*, ITC publication, No. 21, p. 55-60, The Netherlands.
- Santra P., Chopra U. K. and Chakraborty, D. 2008. Spatial variability of soil properties and its application in predicting surface map of hydraulic parameters in an agricultural farm. *Current Science* 95: 7.

- Schumann, A.W. and Zaman, Q. U. 2003. Mapping water table depth by electromagnetic induction. *Applied Engineering in Agriculture* 19 (6): 675-688.
- Sheets, K. R. and Hendrickx, J. M. H. 1995. Non-invasive soil water content measurement using electromagnetic induction. *Water Resource Research* 31 (10): 2401-2409.
- Soil Survey Division Staff, 1993. *Soil Survey Manual*. US Department of Agriculture Handbook No. 18. US Government Printing Office, Washington.
- SRDI, 1986. *Reconnaissance soil survey reports* (34 volumes). Department of Soil Survey (now SRDI), Dhaka, Bangladesh.
- SRDI, 2007. *Soil physiography map of Bangladesh, 2007*. Soil and Land Classification Survey Section, Soil Resource Development Institute (SRDI), Dhaka, Bangladesh.
- Stafford, J. V. 2000. Implementing Precision Agriculture in the 21<sup>st</sup> century. *Journal of Agricultural Engineering Research* 76: 267-275.
- Sudduth, K. A., Drummond, S. T. and Kitchen, N. R. 2001. Accuracy issues in electromagnetic induction sensing of soil electrical conductivity for precision agriculture. *Computers and Electronics in Agriculture* 31: 239-264.
- Sudduth, K. A., Kitchen, N. R., Wiebold, W. J., Batchelor, W. D., Bollerod, G. A., Bullock, D. G., Clay, D. E., Palm, H. L., Pierce, F. J., Schuler, R. T. and Thelen, K. D. 2005. Relating apparent electrical conductivity to soil properties across the north-central USA. *Computers and Electronics in Agriculture* 46: 263–283.
- Triantafilis, J. and Monteiro Santos, F. A. 2009. 2-Dimensional soil and vadose-zone representation using an EM38 and EM34 and a laterally constrained inversion model. *Australian Journal of Soil Research* 47: 809–820.
- Triantafilis, J. and McBratney, A. B. 1998. Development of a mobile EM sensing system for soil salinity assessment in irrigated cotton fields, p. 61-64. *Proceedings of the Ninth Australian Cotton Growers Research Association Conference, Broadbeach, Queensland, Australia, 12-14 August*.
- Triantafilis, J., Lesch S. M., Kevin, L. and Buchanan S. M. 2009. Field level digital soil mapping of cation exchange capacity using electromagnetic induction and a hierarchical spatial regression model. *Australian Journal of Soil Research* 47: 651–663.
- USG-Birol, *Upazila Soil Guide (land and soil resource utilization guide)*, 2008. Soil survey and interpretation division, Soil Resource Development Institute (SRDI), Bangladesh.
- USG-Mymensingh, *Upazila Soil Guide (land and soil resource utilization guide)*, 2009. Soil Survey and Interpretation Division, Soil Resource Development Institute (SRDI), Bangladesh.
- Viscarra, R. A. and McBratney, A. B. 1998. Laboratory evaluation of a proximal sensing technique for simultaneous measurement of clay and water content. *Geoderma* 85: 19-39.

- Viscarra, R. A., Fouad, Y., and Walter, C. 2008. Using a digital camera to measure soil organic carbon and ion contents. *Biosystems Engineering*, 100 (2): 149-159.
- Vitharana, U. W. A. 2008. Spatial inventory techniques in support of site-specific soil management. PhD thesis, Department of soil management, Ghent University, Belgium.
- Webster, R. and Oliver, M. A. 1990. *Statistical methods in soil and land resource survey*. Oxford University Press, NY.
- Webster, R. and Oliver, M.A. 2001. *Geostatistics for environmental scientists*, p. 271, John Wiley and Sons, Chichester.
- Weller, U., Zipprich, M., Sommer, M., Castell, W. Zu. and Wehrhan, V. 2007. Mapping clay content across boundaries at the landscape scale with electromagnetic induction. *Soil Science Society America Journal* 71: 6.
- Wollenhaupt, N. C., Mulla, D. J. and Gotway, C. C. A. 1997. Soil sampling and interpolation techniques for mapping spatial variability of soil properties. In: Pierce, F.J. and Sadler, E. J., editors, *The state of site specific management for agriculture*, p. 19-54. American Society of Agronomy, Crop Science of America and Soil Science Society of America.
- Zhu, J., Morgan, C. L. S., Norman, J. M., Yue, W. and Lowery, B. 2004. Combined mapping of soil properties using a multi-scale tree-structured spatial model. *Geoderma* 118: 321-334.

## 9. Appndices

### Appendix I. Electromagnetic induction (EMI) principal and procedure of EM38 sensor

The EM-38 has had considerable application for agricultural purposes because the depth of measurement corresponds to the root zone. The sensor operates at a frequency of 14.6 kHz and measurements can be made with the instrument dipoles either in horizontal or vertical orientation. The measured EC<sub>a</sub> will be denoted as EC<sub>a</sub>-H and EC<sub>a</sub>-V. In the horizontal orientation both transmitter and receiver coils are oriented parallel to the earth's surface, while in the vertical orientation both coils are perpendicular to the surface. Each orientation has its own depth-response profile, the response curve (Figure 25) describe the relative contribution to the secondary magnetic field arising from a thin horizontal layer at any normalized depth  $z$  (with  $z$  being the depth divided by the intercoil spacing). The response peaks between 0.3 and 0.5 m depth for EC<sub>a</sub>-V, while the surface soil only makes a very small contribution to the secondary field. At 1.5 meter depth the soil still contributes significantly. The response curve of horizontal orientation shows a complete different behaviour with the largest contribution from the near surface soil, monotonically decreasing with depth (McNeill, 1980). However, the strength of the sensor signal is a function of influencing soil parameters like amount of charge on the clay particle, clay content, concentrations of salts in the soil solution and soil moisture content. The more conductive the soil composition, the higher the EC<sub>a</sub> reading indicated by the sensor. Mobile EC<sub>a</sub> measurement equipments have been developed for electromagnetic (EM) geophysical approaches. An EM-38 unit has been developed that carry sensor on a non-metallic sled pulled by a vehicle or tractor. These sleds allow continuous EC<sub>a</sub> measurements but in only one dipole position (Freeland et. al., 2002).

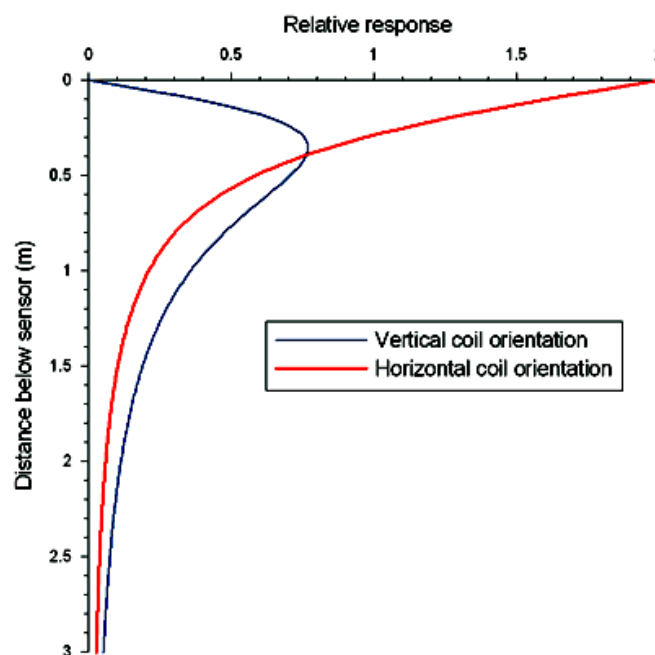


Figure 25. Relative response of EM38 with depth, in two orientations (ORBit, 2010)

Hendrickx and Kachanoski (2002) described the fate of current loops from the sensor, a transmitter coil located at one end of the EM instrument induces circular eddy-current loops in the soil with the magnitude of these loops directly proportional to the electrical conductivity in the vicinity of that loop. Each current loop generates a secondary electromagnetic field that is proportional to the value of the current flowing within the loop. A fraction of the secondary induced electromagnetic field from each loop is intercepted by the receiver coil of the instrument and the sum of these signals is amplified and formed into an output voltage which is related to a depth-weighted soil electrical conductivity (Figure 26). The amplitude and phase of the secondary field will differ from those of the primary field as a result of soil properties, spacing of the coils and their orientation, frequency and distance from the soil surface.

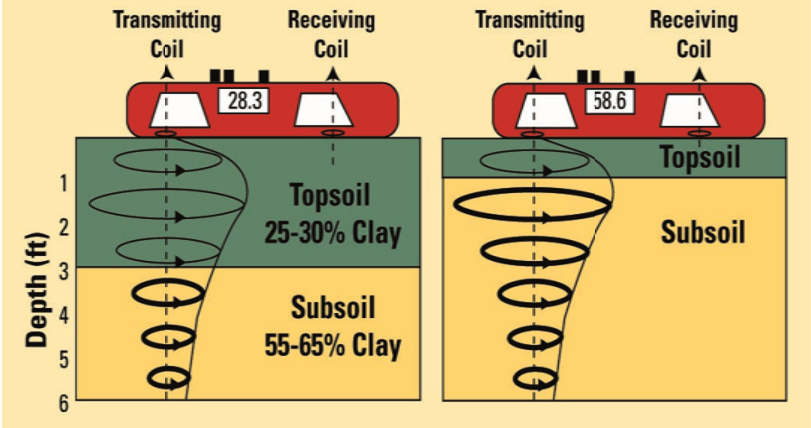


Figure 26. Schematic showing of the operation of EM38 soil conductivity sensor in vertical dipole mode over deep and shallow topsoil (ORBit, 2010).

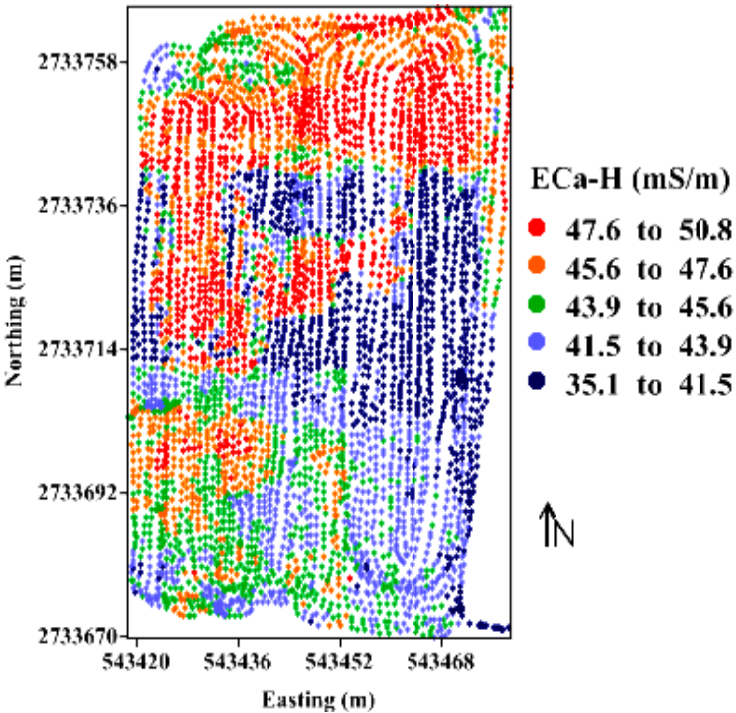
## **Appendix II. Features of a Floating Soil Sensing System (FloSSy)**

In order to acquire high resolution soil data efficiently at wet field conditions, a Floating Soil Sensing System (FloSSy) was developed. Consequently, the FloSSy has to meet the following conditions:

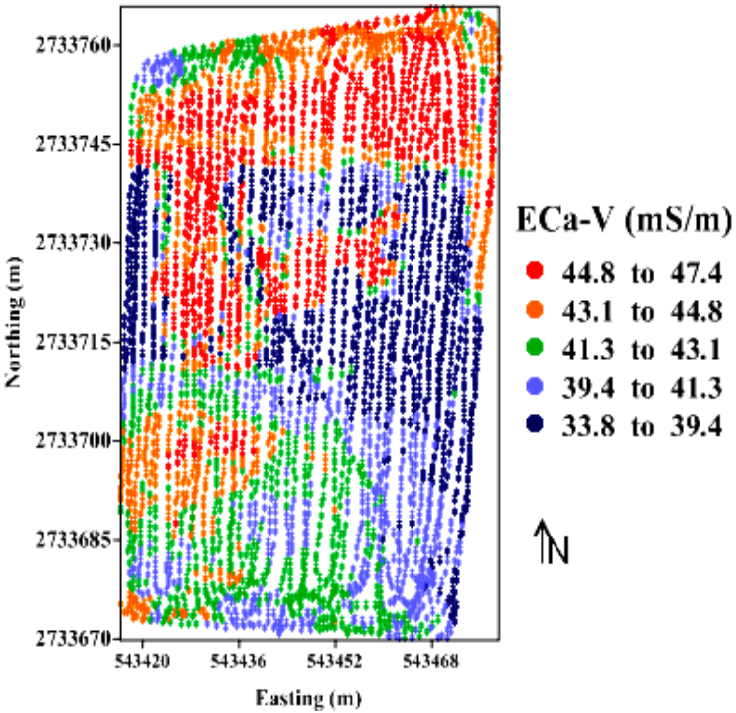
1. The FloSSy should be designed as such that it can be used in flooded fields even under seasonal rainy conditions. Therefore, the housing for all electronics and communication cables must remain waterproof.
2. The system should have a GPS to provide the geographic locations of the recorded soil measurement.
3. The FloSSy should be able to simultaneously process real time raw ECa and GPS information and convert those to the format required by the user. This requires a software component, the FloSSy processor, to function at fully automated on-the-go mode.
4. The FloSSy processor must display the traversing path of the sensor in real time. Otherwise, it will be impossible in a flooded field to track the previously measured path in order to keep a constant distance between measured lines.
5. The sensor carrying platform should be built with light weight material that can float on water. At the same time it should be stable enough against water waves to prevent accidental turning over.

As such, the FloSSy consists of an EMI soil sensing instrument (EM38), a GPS, a field laptop, a real time sensor data processing and path guidance software, a waterproof housing for the soil sensor, a floating platform for the sensor and the GPS and a wetland cultivar vehicle to pull the entire sensing platform on water (Islam, 2009).

Appendix III. a) ECa-H and b) ECa-V measurement points ( $\text{mS m}^{-1}$ ) in the floodplain site



(a)



(b)

**Appendix IV. Critical limits of soil nutrients set by Bangladesh Agricultural Research Council (BARC), Ministry of Agriculture, Bangladesh.**

Table 15. Loamy to clayey soils of wetland rice crops

<b>Nutrient element</b>	<b>Very Low</b>	<b>Low</b>	<b>Medium</b>	<b>Optimum</b>	<b>High</b>	<b>Very high</b>
N (%)	< 0.09	0.091-0.18	1.181-0.27	0.271-0.36	0.361-0.45	>0.45
P (µg/g)	< 3.75	3.76-7.5	7.6-11.25	11.26-15.0	15.1-18.75	>18.75
K (meq/100g)	< 0.075	0.076-0.15	0.151-0.225	0.226-0.30	0.31-0.375	>0.375
Ca (meq/100g)	< 1.5	1.51-3.0	3.1-4.5	4.51-6.0	6.1-7.5	>7.5
Mg (meq/100g)	< 0.375	0.376-0.75	0.751-1.125	1.126-1.5	1.51-1.875	>1.875

Table 16. Classes of organic matter (OM) content and Cation exchange capacity (CEC)

<b>Class</b>	<b>Organic matter (%)</b>	<b>Cation exchange capacity (meq/100 g)</b>
Very high	>5.5	>30
High	3.5-5.5	16-30
Medium	1.8-3.4	7.6-15
Low	1.0-1.7	3-7.5
Very low	<1.0	<3

Table 17. Classes of soil reaction

<b>pH</b>	<b>Soil reaction class</b>
<4.5	Very strongly acidic
4.6-5.5	Strongly acidic
5.6-6.5	Slightly acid
6.6-7.3	Neutral
7.4-8.4	Slightly alkaline
8.5-9.0	Strongly alkaline
>9.0	Very strongly alkaline